https://doi.org/10.5194/egusphere-2026-1464
Preprint. Discussion started: 22 May 2026

Assessing spatially distributed snow simulations with MEB-Crocus in subalpine forests through modelling experiments

Giulia Mazzotti[1,2], Félix Vaccaro[2], Antoine Courteaud[2], Mathieu Fructus[2], Jan Magnusson[3], Isabelle Gouttevin[2], Jari-Pekka Nousu[1,4], Matthieu Lafaysse[2]

[1] Université Grenoble Alpes, INRAE, CNRS, IRD, Grenoble INP, IGE, Grenoble, France
[2] Météo-France, CNRS, Univ. Grenoble Alpes, Univ. Toulouse, CNRM, Centre d'Études de la Neige, Grenoble, France
[3] WSL-Institute for Snow and Avalanche Research SLF, Davos, Switzerland
[4] Natural Resources Institute Finland (Luke), Bioeconomy and Environment, Helsinki, Finland

Correspondence to: Giulia Mazzotti (giulia.mazzotti@inrae.fr)

Abstract. The growing use of physics-based snow models at sub-kilometric resolution for scientific and operational applications calls for spatially distributed model evaluations. Such are particularly challenging in forested areas, where suitable ground truth data is largely lacking. This study assesses the first spatially distributed simulations of the forest snow scheme MEB-Crocus at 250 m resolution through comparison with a benchmark model, FSM2oshd. MEB-Crocus will be integrated in Météo-France's operational snow modelling chain in the near future. Its canopy implementation is based on principles typical for land surface models intended for coarse-resolution large-scale applications, while the canopy implementation in FSM2oshd was specifically developed and validated for simulations in alpine terrain and at sub-kilometric resolution. FSM2oshd has already been successfully evaluated against spatial observations and vegetation parameters were upscaled from hyper-resolution snow-vegetation simulations, providing confidence for using it as a benchmark. A suite of modelling experiments with varying combinations of vegetation datasets and grid cell tiling was performed to enable assessment of different aspects of MEB-Crocus. In the default operational configuration, MEB-Crocus was found to overestimate snow water equivalent (SWE) at peak of winter especially at elevations where forest is present, but to simulate shorter snow cover durations than FSM2. Land cover datasets and process parametrizations accounted for a similar share of model discrepancies. With identical forest structure information, differences in canopy snow processes were the main driver of model discrepancies, with MEB-Crocus generally overestimating peak SWE especially in denser forests. Simulations with MEB-Crocus including recent enhancements to the parametrizations of canopy snow interception and unloading led to strongly reduced differences in peak SWE. Insights from these model comparisons inform future model development efforts and encourage the evaluation of spatially distributed models across a range of forest structures, topographic settings, and meteorological conditions.

https://doi.org/10.5194/egusphere-2026-1464
Preprint. Discussion started: 22 May 2026

1 Introduction

Many of the world's mountain regions host seasonal snow over several months each year, making it a key component of mountain climate, hydrology, and ecosystems. Societies and economies in these regions rely on snow in many ways, which drives a strong interest in snow monitoring efforts from a variety of stakeholders (Bartelt and Lehning, 2002; Hou et al., 2025; Spandre et al., 2019a). Operational monitoring of seasonal snow is thus common in Alpine countries. The corresponding frameworks may differ in terms of data requirements and model complexity, as they serve a wide range of purposes from avalanche forecasting to hydropower management and flood prevention (Avanzi et al., 2023; Morin et al., 2020; Mott et al., 2023; Olefs et al., 2020). Yet, they mostly involve a modelling component to continuously track and predict the evolution of snow state variables, complementing spatially and temporally discrete observations. Thanks to widespread recent advances in computational resources and continued progress in the spatial resolution of available meteorological products, there is a strong push towards fully distributed, mass- and energy-based snow models at increasingly high resolutions (Lute et al., 2022; Marsh et al., 2020; Reynolds et al., 2024; Strasser et al., 2024). However, applications of such models over the extents of full mountain ranges or watersheds usually span multiple land cover types and require a realistic representation of how these interact with snow on the ground. In forested terrain, this involves numerous processes by which forest canopies alter fluxes of mass and energy to the snowpack on the forest floor, such as snowfall interception, radiation transfer, and wind attenuation (Bonner et al., 2022; Kraft et al., 2022; Mazzotti et al., 2020b), which adds to model complexity and input data needs.

Model evaluation is also particularly challenging in forests, due to the scale gap between measurements, process variability, and model resolution (Broxton et al., 2021; Clark et al., 2011; Mazzotti et al., 2021). Traditionally, forest snow model validations have only involved point simulations at few sites (Bouchard et al., 2024b; Essery et al., 2009; Napoly et al., 2020; Nousu et al., 2024). Spatially distributed applications, however, also require spatially explicit model evaluations. In fact, point evaluations at station locations are usually limited to flat terrain and may miss systematic model errors linked to terrain features or land cover characteristics (Cluzet et al., 2024). In view of application over large areas, the impact of such systematic errors on the assessment of snow water resources is key (Berg et al., 2024). Novel satellite products offer exciting opportunities to yield validation data for this purpose (Barnhart et al., 2024; Sourp et al., 2025). Yet, again, forest terrain poses particular challenges due to the occlusion of most remote sensing technologies, causing high uncertainties in the associated products in these areas (Gascoin et al., 2019; Notarnicola, 2020). To date, LiDAR remains the only technology to deliver reliable information on the snow cover below forest canopies (Currier et al., 2019; Deschamps-Berger et al., 2023; Gascoin et al., 2024). However, large-scale, high-resolution and repeat LiDAR acquisitions have so far only been conducted over Western American watersheds (Painter et al., 2016), while equivalent datasets are inexistent over European mountain forests. Assessing forest snow model performance at landscape scales thus still represents a major research gap: Only very few studies have specifically targeted spatially distributed model evaluations of forest snow at typical operational resolutions (Haagmans et al., 2025; Smyth et al., 2022). Recent advances in spatially distributed forest snow models have rather focused

https://doi.org/10.5194/egusphere-2026-1464
Preprint. Discussion started: 22 May 2026

on small areas and very high spatial resolutions, while comprehensive evaluations of models intended for larger scale are usually still done at the point or site scale (Förster et al., 2018; Mazzotti et al., 2021). However, given that forests, snow, and mountains, overlap over substantial portions of the Northern Hemisphere, including the European Alps (Deschamps-Berger et al., 2025), the challenges associated with spatial large-scale applications of forest snow models outlined above should not be overlooked; all the more as hydrological assessments, which are a key application of such models, intrinsically rely on a spatial representation of snow.

In this study, we address the performance of the new and distributed forest snow model MEB-Crocus by focusing on seven years of simulations over a study area in the Swiss Alps at 250m spatial and daily resolution, which corresponds to that of the future operational snow modelling system covering all French mountain areas (Haddjeri et al., 2024). MEB-Crocus is the recent coupling of the detailed Crocus snowpack scheme (Lafaysse et al., 2025) with an explicit vegetation layer (Boone et al., 2017) within the SURFEX land surface modelling platform used operationally at Météo-France. While forest snow simulations with MEB have already been evaluated at the point scale (see Sect. 2.1), simulations conducted for this study represent a first spatially distributed application over complex terrain. MEB-Crocus results are assessed against simulations conducted with FSM2oshd, the Swiss operational snow hydrological model (Mott et al., 2023), which is here considered as benchmark. This is justified by the robust agreement between FSM2 and hyper-resolution snow-vegetation simulations at the point scale, as well as existing spatial evaluations of FSM2oshd (see Sect. 2.2). The use of a benchmark model further allows considering more variables than snow distribution alone.

A series of model experiments applying MEB-Crocus in different configurations are performed to address the following research questions:

1. How can a benchmark model be best used to assess the performance of new spatially distributed snow model simulations in complex forested landscape?
2. How do forest snow dynamics simulated by the two models differ across complex topography, varying forest density, and variable meteorological conditions, and which model parameters and processes drive these differences?
3. How large is the impact of vegetation structure data relative to process representation on simulated forest snow dynamics?
4. What do these findings imply for future model development priorities?

While this study is primarily motivated by the prospective use of MEB-Crocus for operational snow modelling at Météo-France, its outcomes are relevant in a wider context. Scientific applications of Crocus and SURFEX are plenty and span a broad range of science fields (Roussel et al., 2025; Spandre et al., 2019b; Woolley et al., 2024). Notably, the current semi-distributed snow and meteorological reanalysis S2M (Vernay et al., 2022) is now widely used as reference for snow conditions over the French Alps (Kneib et al., 2024; Le Roux et al., 2023; Michalet et al., 2024; Roussel et al., 2024); a future update of this product using the fully-distributed model version, of which will also include forest effects, would be the basis of follow-up research, requiring thorough knowledge of the strengths and limitations of such a product. Moreover, the

https://doi.org/10.5194/egusphere-2026-1464
Preprint. Discussion started: 22 May 2026

recent developments of MEB-Crocus and its spatially distributed high-resolution application are exemplary of other land surface models (LSM) such as Noah-MP, CLM, and SVS2 (He et al., 2023; Lawrence et al., 2019; Vionnet et al., 2025). Ongoing evaluation efforts of these models may thus benefit from the lessons learnt using the forest snow model evaluation approach proposed here.

2 Data and Methods

2.1 The model of interest: MEB-Crocus scheme within SURFEX

Operational monitoring and forecasting of snow and avalanche conditions in French mountains is handled by Météo-France since the 1990s, with the detailed snow physics model Crocus (Brun et al., 1992) being at the core of this effort. Crocus is a high complexity, physics-based snow model that tracks the evolution of the snow state variables depth, density, liquid water content, temperature, age, and microstructure descriptors for a maximum of fifty snow layers by resolving heat diffusion and liquid water transport within the snowpack, snow compaction, and metamorphism. Lafaysse et al. (2025) present the evolution laws of these state variables in detail, as well as the numerical assumptions for coupling Crocus with the other components of the SURFEX LSM, i.e. the ISBA-DIF soil model (Decharme et al., 2016) and the MEB vegetation scheme (Boone et al., 2017).

Crocus is used in Météo-France's current operational modelling chain S2M (SAFRAN–SURFEX/ISBA–Crocus–MEPRA), which has been used to produce today's reference reanalysis datasets of long-term snow and meteorological conditions in French mountain areas (Vernay et al., 2022). The current semi-distributed model setup disregards forest, and validation efforts have thus so far focused on open areas (Revuelto et al., 2018; Viallon-Galinier et al., 2020). Yet, an upcoming update of the snow modelling chain, expected to become operational within a few years, foresees a switch to a distributed spatial representation with a 250m resolution, which will also require representing forested areas.

First efforts to apply Crocus to forested areas have been made within the SURFEX platform. An explicit, one-layer vegetation representation option called MEB ('Multi-Energy-Balances') was implemented in ISBA by Boone et al. (2017). The canopy layer is coupled to the below-canopy ground via a canopy air space (which is also the case for FSM2oshd, see Sect. 2.2). As in many LSMs, the canopy is assumed to be a homogeneous layer and described in terms of canopy height and Leaf Area Index (LAI). MEB is coupled to the snow schemes available in ISBA and has mainly been used with the ES ('Explicit Snow') option (Napoly et al., 2020). Coupling with Crocus was presented by Vincent et al. (2018), including first evaluation at the point scale, and documented in detail by Lafaysse et al. (2025); other point-scale evaluations were done in the context of ESM-SnowMIP (Krinner et al., 2018) and at Finnish sites in the study by Nousu et al. (2024). While the results of these evaluations were generally promising, Vincent et al. (2018) identified weaknesses in representing canopy snow processes in Alpine regions. Developments to improve canopy snow interception and unloading parametrizations have been ongoing at Météo-France in parallel to and independent of the present study, but are not yet included in an official

https://doi.org/10.5194/egusphere-2026-1464
Preprint. Discussion started: 22 May 2026

release. A publication describing these updates and their evaluation with experimental data at instrumented sites is in preparation (Pauze et al. in prep.). Meanwhile, a description is provided in the Supporting Information.

In 1-D simulations with SURFEX, as in many other LSMs that enable point simulations, site-parameters such as forest structure descriptors can be defined manually by the user. Usually, this information is available from in-situ measurements, as e.g. in the SnowMIP2 intercomparison experiment, (Essery et al., 2009). For 2-D applications, this is unfeasible, and parameter databases are used instead. For simulations over Europe, SURFEX relies on the surface cover database ECOCLIMAP-II (Faroux et al., 2013), which includes an ecosystem classification and the corresponding set of land surface parameters at 1 km resolution over all of Europe (referred to as ECOCLIMAP in the following for simplicity). Sub-grid variability of surface covers is treated with a nested tiling system. For coarse-resolution applications of SURFEX, including climate modelling (Monteiro et al., 2024a), a grid cell can contain multiple surface types such as 'town', 'water' or 'nature', treated with different models. Snow is represented within the tile nature, which is handled by the ISBA LSM. The nature tile can contain a maximum of 19 land cover types, referred to as patches. These represent various land covers from bare rock to grassland and low vegetation to different forest types, characterized by specific values of land surface and vegetation descriptors such as LAI and tree height. ISBA can be run separately for each patch, or for a user-defined limited number of patches, in which case land surface descriptors are averaged. For this study, we lumped all land cover characteristics into one patch, as any other approach would be too expensive in an operational setting that typically faces computational constraints and because the need to split grid cells into various land cover types decreases at high spatial resolution. The resampling of ECOCLIMAP data to the 250m resolution is handled by SURFEX. It is also possible to provide external surface parameter grids to SURFEX to override the ones derived from ECOCLIMAP, an option we used for some of our simulations (see Sect. 2.4).

2.2 The benchmark model: FSM2OSHD framework

The operational snow-hydrological model used in Switzerland, FSM2oshd (Mott et al., 2023) has evolved from the intermediate-complexity snow model FSM2 (Essery, 2015; Essery et al., 2025; Mazzotti et al., 2020a). As Crocus, FSM2 is mass- and energy balance based, but the snowpack is represented with few (numerical) layers only and snow metamorphism is not included. Contrary to Crocus, FSM2oshd is not embedded in a full LSM but only coupled to a simple soil routine that mainly serves to define lower snowpack boundary conditions. The model runs operationally at 250m resolution over entire Switzerland and neighboring watersheds, driven by meteorological forcing issued from the COSMO numerical weather prediction model and downscaled to the target resolution (Mott et al., 2023), as well as data assimilation steps, notably the assimilation of snow station data to correct precipitation fields (Magnusson et al., 2014).

In establishing FSM2oshd, a particular effort was put into an implementation of forest snow processes tailored to its resolution. Process representations were developed and validated at the point scale (or 'hyper-resolution') to enable direct evaluation with point measurements of both snow distribution (Mazzotti et al., 2020a) as well as individual energy exchange processes (Mazzotti et al., 2020b). While these parametrizations relied on very local canopy structure descriptors, subsequent

https://doi.org/10.5194/egusphere-2026-1464
Preprint. Discussion started: 22 May 2026

work explored how these representations scale up to resolutions coarser than the typical forest snow process scales (Mazzotti et al., 2021). Based on these findings, canopy structure datasets were developed for the FSM2oshd framework from a high-resolution (1m) canopy height model created from airborne LiDAR and information on forest types. Local metrics calculated at 10m spacing using the model CanRad (Webster et al., 2023) were averaged to provide grid-cell-level values. The dataset is presented in Webster et al. (2025) and we will refer to it as the CanRad vegetation data for simplicity. Unlike SURFEX, FSM2oshd distinguishes only four surface types: open terrain, glacier surfaces, forests, and water bodies. Separate instances of FSM2oshd are run for each surface type, except for the water fraction, where it is assumed that no snow cover develops. These separate model runs are independent of the grid cell fraction occupied by each surface cover type. To account for the co-occurrence of multiple surface types in one grid cell, grid-cell-level values are then obtained as a weighted average of the model outputs from each instance, where weights correspond to the fraction of the grid cell occupied by each land cover type. By default, the instance representing open terrain is run over the entire domain, even on grid cells that are fully occupied by the three other land cover types. Note that the presence of glaciers and water bodies is negligible over our study domain.

Although the FSM2oshd framework is being continuously developed further, a few years of reference simulations have already become available since its establishment. Of particular relevance for this study, Haagmans et al. (2025) assessed FSM2oshd runs in forested complex terrain against Planetscope imagery that was processed manually to determine snow cover fractions in forested and non-forested grid cell portions. This evaluation included ~30'000 manually evaluated validation points and is, to the best of our knowledge, the only available validation for forest snow simulations across such extents in the European Alps. In summary, considering existing extensive evaluation efforts at the point scale (Mazzotti et al., 2023, 2020a, 2020b), analysis of model upscaling behavior (Mazzotti et al., 2021), and the plausibility assessment against satellite imagery at operational resolution (Haagmans et al., 2025), all of which happened within the study area considered in this study, we regard FSM2oshd as a legit benchmark against which to assess MEB-Crocus in view of its application to modelling forest snow water resources across the French Alps.

https://doi.org/10.5194/egusphere-2026-1464
Preprint. Discussion started: 22 May 2026

2.3 Study area, period, and input datasets

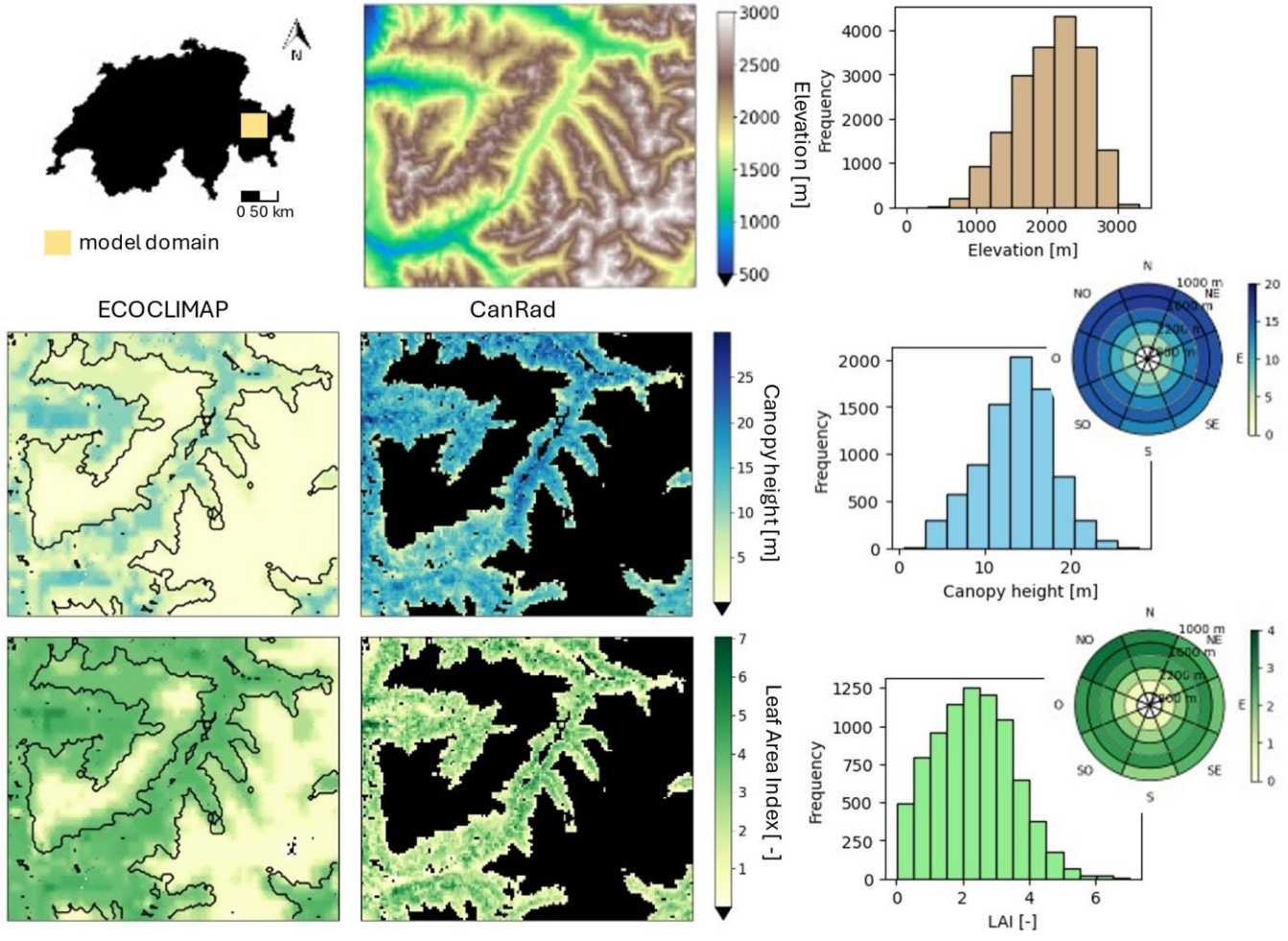

Figure 1: *Overview of the study domain. Location within Switzerland, elevation map and corresponding frequency distribution (upper row), as well as data of canopy height (center row) and leaf area index (LAI, bottom row) according to ECOCLIMAP (left) and CanRad (center); frequency distribution of the CanRad datasets and average values binned by 300m elevation and 45 aspect class (right).*

We conduct model comparisons over a geographic domain located in the Eastern Swiss Alps (Fig 1.) and driven by identical meteorological forcing, which allows to fully attribute differences between simulations to the model. The study area comprises 37.5 by 32 km (126x149 = 18774 grid cells) and corresponds to the model domain considered by Quéno et al. (2024), and to one of the domains analyzed by Haagmans et al. (2025). Elevations range from 540 to 3417 m, meaning seasonal snow is present in most of the domain, whereas the snowpack is ephemeral in the remaining parts. The domain covers all orientations and representative slope classes, and contains forest types typical for the Alpine region. Forests with substantial seasonal snowpacks are all mostly needleleaf, largely evergreen but containing a minor fraction of deciduous trees in the south-east of the domain. Some deciduous broadleaf forests are found in the north-west of the domain. According

https://doi.org/10.5194/egusphere-2026-1464
Preprint. Discussion started: 22 May 2026

to the CanRad dataset, 40% of the grid cells in the model domain are at least partially covered by forest. Forest densities vary, with LAIs in the range of 0 to 7, and canopy heights reach up to 25m. As seen in the polar plots of Fig. 1, canopy characteristics are approximately homogeneous across aspects, however there is a tendency for the canopy to become sparser with increasing elevation.

Meteorological forcing is obtained through the OSHD modelling framework, to maintain consistency with the reference FSM2oshd runs described in Section 2.2. Hourly fields of precipitation, short- and longwave radiation, air temperature, humidity and pressure, as well as wind speed, are available from the COSMO model at 1km resolution and downscaled to the model resolution of 250m applying downscaling algorithms described in Mott et al. (2023). Precipitation input is partitioned into solid and liquid fractions, and corrected through assimilation of snow station data, also described in Mott et al. (2023). We consider seven hydrological years (WYs), with simulations spanning 1. September 2016 to 31. August 2023, which allows testing whether inter-annual variability of meteorological conditions affects the consistency of our findings.

2.4 Model experiments

Our model experiments use different simulations from the two models to generate a set of output configurations which each serves a different purpose. An overview, including the naming conventions used in the rest of this article, is provided hereafter and illustrated in Fig. 2.

The simulations and corresponding outputs are characterized as follows:

0. FSM2oshd benchmark: These model outputs were available through SLF's operational snow hydrological service and Haagmans et al. (2025). Thank to FSM2oshd's tiling strategy, three different output configurations can be leveraged for this study: The outputs from model instances representing open and forested terrain (FSM_opn and FSM_for, respectively) as well as the grid-cell-scale output created based on the former two and accounting for both forested and open grid cell fractions (FSM_all).
1. MEB-Crocus default simulation (MEBCro_def): This simulation uses the default MEB-Crocus configuration as available in SURFEX, with vegetation parameters extracted from the ECOCLIMAP database.
2. Crocus open terrain simulation (Cro_opn): This simulation disregards vegetation to mimic open terrain by setting LAI and vegetation height to zero over the entire domain, and therefore also does not include MEB. This simulation is thus the Crocus equivalent of FSM_opn.
3. MEB-Crocus forest-only simulation with CanRad data (MEBCro_for): In this simulation, LAI and canopy height fields from the CanRad vegetation data were provided to SURFEX, replacing ECOCLIMAP datasets. All grid cells with non-zero LAI and canopy height values were assumed to be fully forest covered. This simulation is thus the MEB-Crocus equivalent of FSM_for.
4. MEB-Crocus with CanRad vegetation data and accounting for forested and open grid cell fractions (MEBCro_all): This model output is derived by combining the simulations Cro_opn and MEBCro_for, where values assigned to

https://doi.org/10.5194/egusphere-2026-1464
Preprint. Discussion started: 22 May 2026

each grid cell are computed as the weighted average of these two runs and the weights are given by the grid cell fractions occupied by open and forested terrain, respectively. This simulation is thus the MEB-Crocus equivalent of FSM_all.

5. MEB-Crocus forest-only simulation with CanRad data and recent model extensions (MEBCroXT_for): This simulation is similar to MEBCro_for, but additionally includes the improved canopy snow routines from Pauze et al. (in prep).

6. MEB-Crocus output with CanRad vegetation data, recent extensions, and accounting for forested and open grid cell fractions (MEBCroXT_all): This simulation is created equivalently to MEBCro_all, but using the MEBCroXT_for simulation instead of the MEBCro_for one for the forested grid cell fractions.

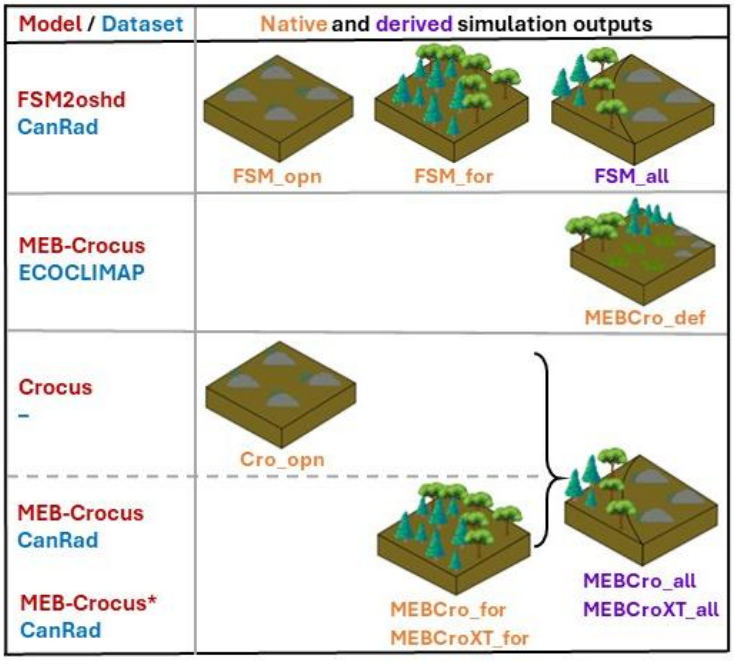

Figure 2: *Summary of model experiments, showing the different combinations of models, forest datasets, and grid cell tiling, and including both direct (native) outputs as well as those derived by combining multiple native outputs. The asterisk refers to the version of MEB-Crocus including the unpublished enhancements to the canopy snow module.*

2.5 Evaluation strategy

The aim of our approach is to obtain insights into specific aspects of MEB-Crocus performance by comparing outputs from different model experiments to the FSM2oshd simulations. To summarize the evolution of snow cover during each season, we considered metrics based on snow water equivalent (SWE [mm], corresponding to [kg m^{-2}]) defined as in Mazzotti et al. (2023) and visualized in Fig. 3.

https://doi.org/10.5194/egusphere-2026-1464
Preprint. Discussion started: 22 May 2026

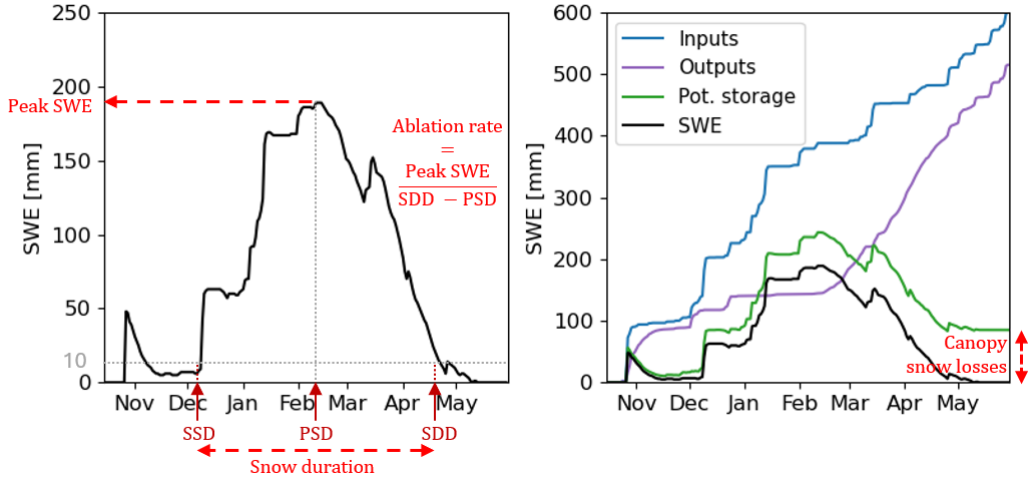

Figure 3: *Illustration of snow season descriptors considered for the analysis, based on snow water equivalent (SWE). The potential storage in the right panel is computed as difference between inputs and outputs, the difference between potential storage and SWE at any point in time represents the cumulative canopy snow loss up to this point.*

- Peak SWE: Maximum value of snow water equivalent reached during a water year (WY). The day of peak SWE occurrence is referred to as peak SWE day (PSD).
- Snow cover duration: Number of days between the start of the snow season (SSD), defined as the day after the last occurrence of SWE <10 mm prior to peak SWE, and the day of snow disappearance (SDD), defined as the last day before the first occurrence of SWE < 10 mm following peak SWE.
- Ablation rate: The quotient between peak SWE and the length of the ablation period, computed as SDD-PSD

For simulations focusing on the forest, we further considered descriptors aimed at characterizing specific, canopy-influenced processes. We included descriptors characterizing both accumulation and ablation processes, and limited our analysis to processes that are largely influenced by the canopy only, with very minimal impact of the properties of snow on the ground.

- Canopy snow losses: intended to quantify forest impacts on accumulation processes, these were calculated as the difference between water inputs (snowfall and rainfall) and outputs (melt and sublimation of snow on the ground), with respect to sub-canopy SWE, over the entire WY. This metric thus quantifies the net impact of interception in the canopy and subsequent partitioning into unloading to the ground and sublimation losses.
- Sub-canopy radiation components: intended to quantify forest impacts on ablation processes, sub-canopy incoming short- and longwave radiation components were considered, representing a major energy input to the subcanopy snowpack. These processes are independent of the snow conditions simulated by the two models, as neither of the two models account for the presence of intercepted snow in their parametrization. Daily values as well as the average for the month of March (which constitutes an important phase of the ablation period in the forests of our study domain) were considered.

https://doi.org/10.5194/egusphere-2026-1464
Preprint. Discussion started: 22 May 2026

All metrics described above were calculated for all simulations, every grid cell within the model domain, and separately for each WY. However, given the many dimensions involved in our analysis (multiple simulations, thousands of grid cells with varying topography and forest structure, and daily output of multiple modelled variables over seven hydrological years), a meaningful spatio-temporal aggregation of model results is indispensable. To synthesize the spatial dimension of our model domain, we computed the average of each snow season descriptor within elevation bands spanning 300 m and aspect classes covering 45° each. We limited the analysis to elevations between 1000 and 2800 m, to ensure a sufficient and roughly even number of grid cells with seasonal snow in each of the altitude and aspect classes considered. Additionally, where relevant, we further distinguished forest density classes by aggregating grid cells according to their LAI values. LAI is a suitable parameter to this end as it is used by both models, moreover it is well correlated to canopy height in the CanRad dataset ($R = 0.78$).

Absolute model discrepancies in all our analyses are expressed as difference between the MEB-Crocus simulation in question and the relevant FSM2oshd run, i.e. positive values of a quantity mean MEB-Crocus overestimated this quantity relative to the FSM2oshd benchmark. Relative model discrepancies are expressed as percentage of the FSM2oshd benchmark.

3. Results

3.1 Model differences between the default configurations of MEB-Crocus and FSM2oshd

To set the stage for the subsequent more detailed analysis, we first explore how the two ‘default’ operational configurations of MEB-Crocus and FSM2oshd compare by assessing the simulation MEBCro_def against FSM_all. Figure 4 summarizes this comparison, showing differences in peak SWE (Fig. 4a), snow duration (Fig. 4b) and ablation rate (Fig. 4c) aggregated by elevation bands and aspect classes and averaged over all modelled WYs, computed as MEBCro_def – FSM_all. To visualize the spatial distribution of model discrepancies, peak SWE differences in WY 2020/21 are mapped in Fig. 4d as an example. The temporal evolution of model differences is illustrated by SWE time series in Fig. 4e, showing the mean and interquartile range of all grid cells in the elevation range 1300-2200m.

https://doi.org/10.5194/egusphere-2026-1464
Preprint. Discussion started: 22 May 2026

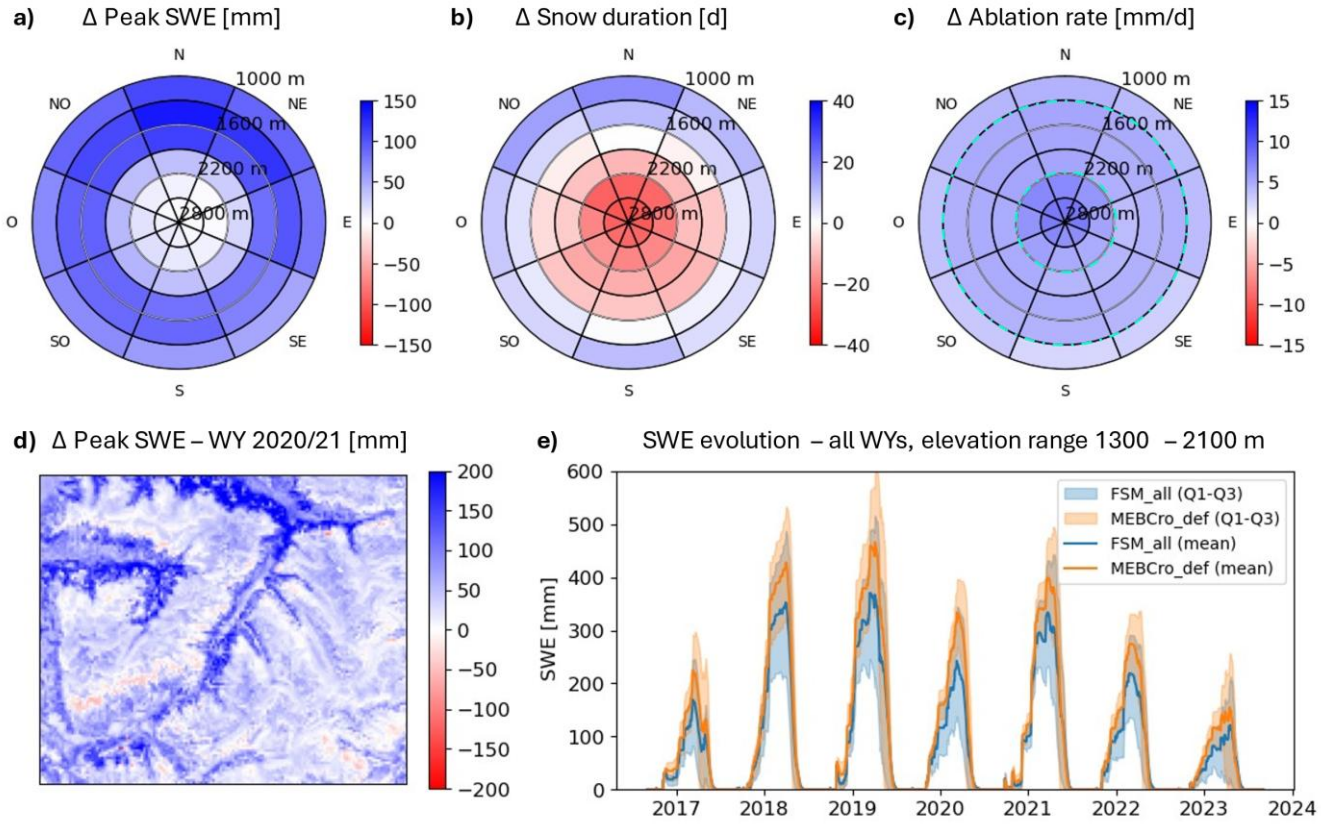

Figure 4: *Differences between MEBCro_def and FSM_all simulations, including peak SWE (a), snow duration (b), and ablation rate (c) aggregated by elevation band and aspect classes and averaged over the seven WYs considered. An example of spatial distribution of model differences is provided in terms of peak SWE in WY 2020/21 (d), and the temporal evolution of SWE differences is illustrated with SWE time series (e), with lines representing the means and shaded areas the interquartile ranges of all grid cells in the elevation range 1300-2200m (between the two cyan dashed lines in panel c).*

MEBCro_all predicts consistently higher peak SWE than FSM_all across all topographic classes, with higher model discrepancies at lower elevations and no marked aspect dependency (Fig. 4a). This positive bias amounts to 46 mm on average, corresponding to ~13% of average peak SWE. Locally and for individual years, discrepancies can exhibit a much wider range (Fig. 4d). Generally, the spatial patterns of model differences reveal these to be larger in the forested areas of the domain (see Fig. 1), while small areas where FSM_all features higher peak SWE than MEBCro_def do exist but are limited to the highest peaks of the model domain (Fig 4d). Although this observation suggests that model differences may be at least partly due to differences in land cover data between the two models, peak SWE differences were found to be only weakly correlated with LAI differences (R = -0.5 on average over all WYs). It is also noteworthy that the two models simulate a similar range of peak SWE spatial variability, as coefficients of variations of peak SWE computed over the same topographic classes were of comparable magnitude (0.27 averaged over all WYs for MEB_def, 0.34 for FSM_all).

https://doi.org/10.5194/egusphere-2026-1464
Preprint. Discussion started: 22 May 2026

MEBCro_def simulates longer snow duration than FSM_all at lower elevations, while the trend is reversed at higher elevations (Fig. 4b). On average, snow cover lasts 11 days longer in FSM_all. This suggests that the larger peak SWE in MEBCro_def is partly compensated by more efficient ablation, which is confirmed by Fig. 4c, revealing faster ablation rates for MEBCro_def regardless of elevation and aspect (Fig. 4c), by 5 mm/d on average. These findings and their temporal consistency are confirmed by the SWE time series shown in Fig. 4e, which show similar relative behavior of the two models in both snow-rich and snow-scarce years.

Given the very different strategies used by the two models to account for sub-grid variability in landcover, these results remain purely diagnostic and cannot be attributed to specific processes at this stage. While providing a baseline in terms of a comparison between the original 'standard' configurations of the two models, they also underpin the need for a more detailed analysis through dedicated model experiments.

3.2 Model differences due to snowpack processes: comparison of runs without forests

Figure 5 presents a comparison of the simulations Cro_opn and FSM_opn, aiming to assess model differences due to the snowpack representation only. While not a focus of this study, such analysis is informative as it provides context to the subsequent analyses, which will focus on forest-specific processes.

Figure 5a-c shows differences in peak SWE, snow duration, and ablation rate, equivalent to Fig. 4a-c. Overall, we find similar tendencies as in Sect 3.1, but with some important differences. Discrepancies in peak SWE are generally small, with Cro_opn simulating greater peak SWE at low elevations, but FSM_opn featuring higher values at high elevations, regardless of aspect. Averaged over all aspects and elevation bands, Cro_opn shows a positive peak SWE bias of 9 mm (corresponding to 2%). Variability in peak SWE was similar for the two models (average coefficient of variation of peak SWE per topographic class: 0.25 for Cro_opn, 0.28 for FSM_opn). Snow duration is longer in the FSM_opn simulations, by 21 days on average, except at elevations below 1600 m and south-facing aspects. Lastly, ablation rates are consistently higher for Cro_opn (6 mm/d on average), where differences to FSM_opn increase slightly with elevation and appear to be larger at north- than at south-facing aspects.

SWE time series provide further insights into these contrasting results. SWE mean and interquartile ranges for the elevation range 1000-1600 m and SE to SW aspect classes are plotted for both Cro_opn and FSM_opn in Fig. 5d. Especially in snow-poor years, Cro_opn achieves considerably larger SWE throughout the season, as well as a later melt onset than FSM_opn. leading to longer snow duration despite the higher melt rates. Comparing the models at individual points located in these terrain classes (not shown) revealed that, besides exhibiting earlier melt onset, FSM_open also appears to be more prone to intermittent melt events early in the season, which partially explains the large discrepancies in peak SWE. In contrast, the time series for the elevation range 2200-2800 m and NW to NE aspect classes shown in Fig. 5e reveal the two models to simulate very similar accumulation and melt onset, but consistently higher ablation rates for Cro_opn, resulting in shorter snow duration. This difference is likely partly due to the different treatment of fractional snow by the two models: The parametrization used by FSM2oshd assumes partial snow cover for larger average snow depths than MEB-Crocus, which

https://doi.org/10.5194/egusphere-2026-1464
Preprint. Discussion started: 22 May 2026

entails a smaller exposed snow surface and may result in slower ablation rates (Essery and Pomeroy, 2004). This important structural difference between the two models thus needs to be kept in mind when interpreting differences in ablation processes.

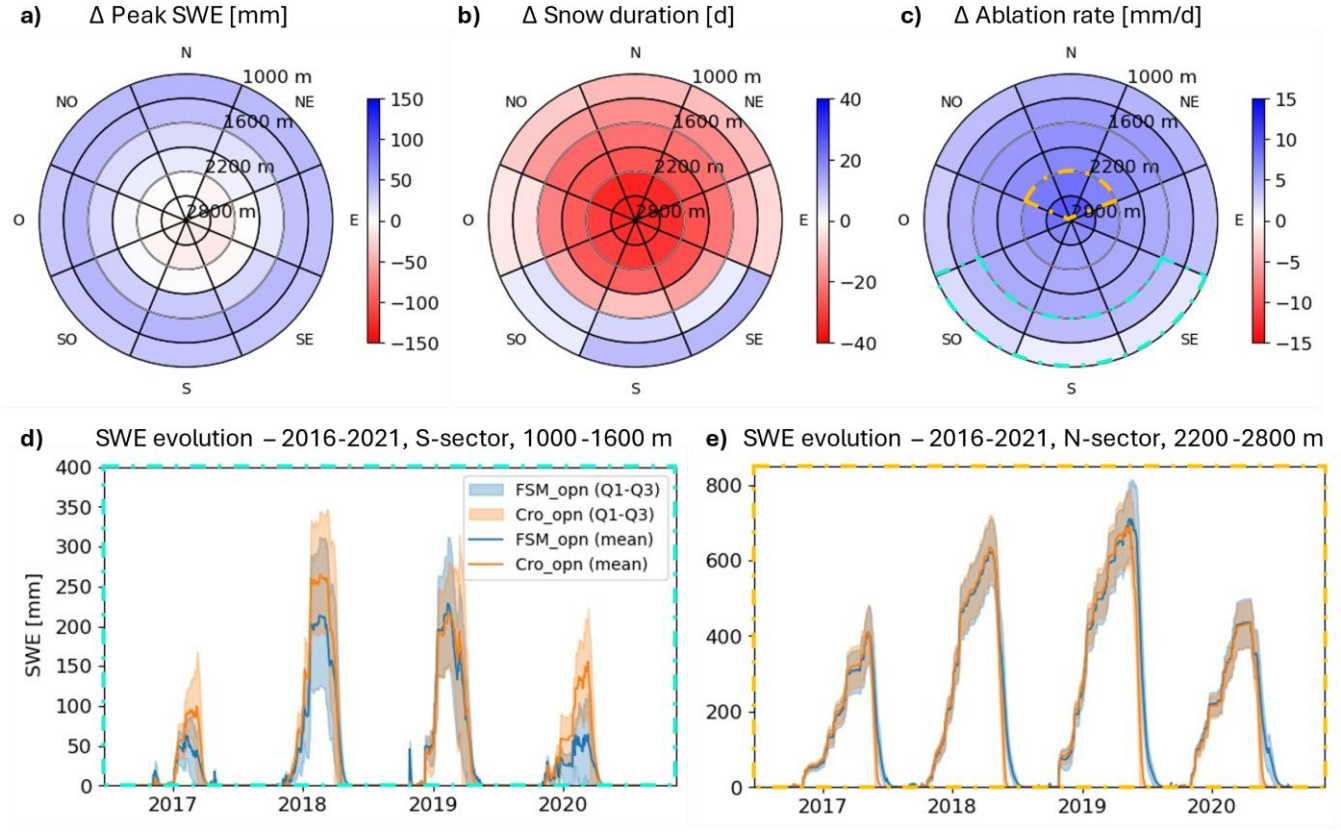

Figure 5: *Differences between Cro_opn and FSM_opn simulations, including peak SWE (a), snow duration (b), and ablation rate (c) aggregated by elevation band and aspect classes and averaged over the seven WYs considered. The temporal evolution of SWE differences is illustrated by SWE time series, with lines representing the means and shaded areas the interquartile ranges of grid cells in the elevation range 1000-1600m and SE to SW facing aspects (d, sector highlighted by cyan dashed line in panel c), and in the elevation range 2200-2800m and including NW to NE aspects (e, orange dashed line in c).*

3.3 Model differences due to forest processes: comparison of runs with identical vegetation

The following section aims to isolate effects of processes modulated by the forest canopy by comparing the simulations MEBCro_for and FSM_for. As detailed in Sect. 2.4, these simulations use identical LAI and canopy height input data and both assume forested grid cells to be fully covered by forest (in FSM2oshd, this corresponds to a forest cover fraction of 1 wherever forest is present in the domain).

The tendency for MEB-Crocus to accumulate more snow, but melt faster and thus exhibit shorter snow duration than FSM2oshd is found with these model configurations as well, as seen in Fig. 6a-c. Peak SWE overestimations by

https://doi.org/10.5194/egusphere-2026-1464
Preprint. Discussion started: 22 May 2026

MEBCro_for relative to FSM_for are stronger than for the model simulations without forest (Sect. 3.2) and for the default configurations (Sect. 3.1), the average bias amounting to 67 mm but exhibiting a slight decrease with elevation. Noteworthily, both models simulate the same degree of peak SWE spatial variability (average coefficient of variation by elevation and aspect class: 0.28). Combined with consistently higher ablation rates, this leads to MEBCro_for also exhibiting consistently shorter snow durations than FSM_for (by 14 days on average), without marked dependence on topography. Because higher elevations also feature sparser forests (see Fig. 1), we further analyzed SWE time series for different LAI classes and two contrasting WYs (Fig. 6d) to explore whether the apparent elevation dependency in Fig 6a might actually reflect a dependency on canopy density. Indeed, we find differences in SWE between the two models to increase with canopy density despite decreasing absolute SWE, both in a snow rich and in a snow poor year, indicating that canopy density impacts outweigh topographic impacts on model discrepancies.

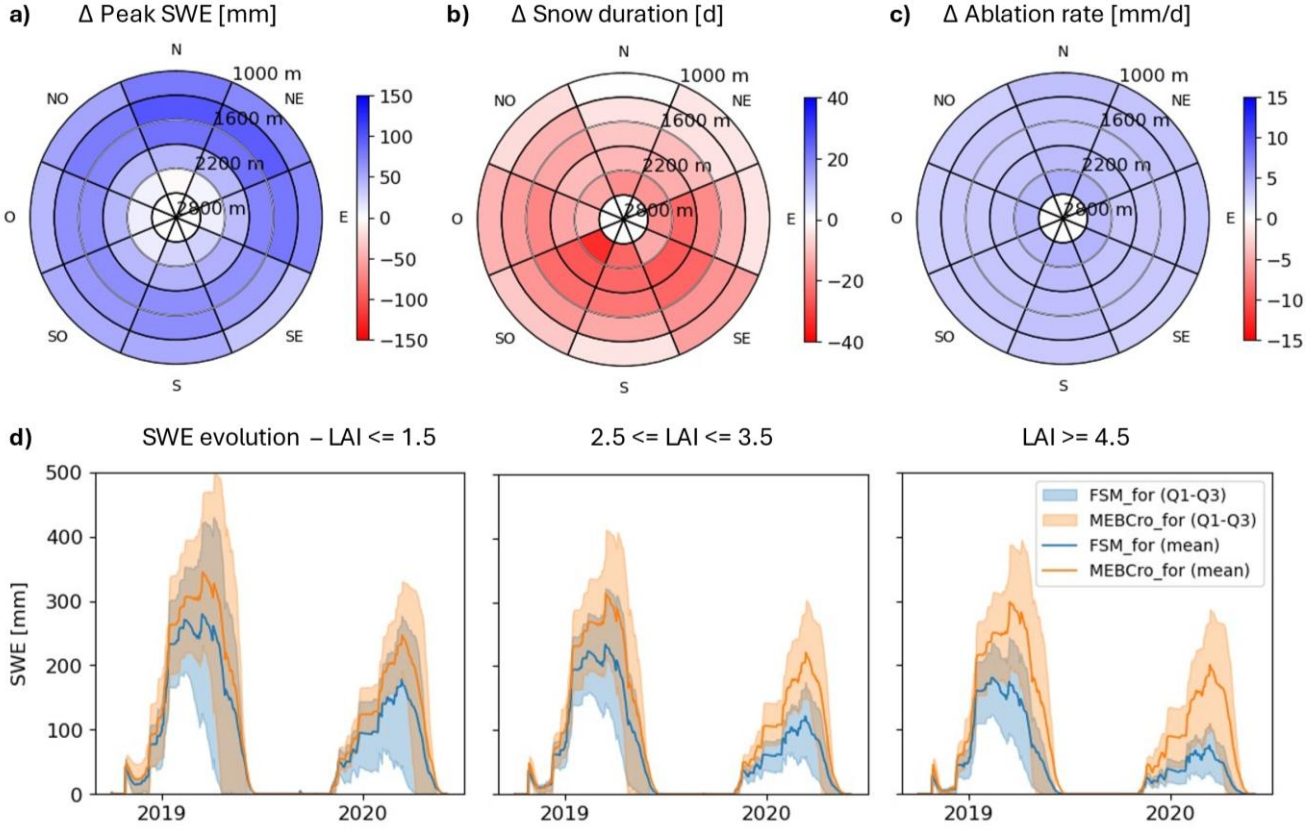

Figure 6: *Differences between MEBCro_for and FSM_for simulations, including peak SWE (a), snow duration (b), and ablation rate (c) aggregated by elevation band and aspect classes and averaged over the seven WYs considered. The temporal evolution of SWE differences is illustrated by SWE time series (d), with lines representing the means and shaded areas the interquartile ranges of grid cells with small (left), medium (center), and large (right) LAI values.*

Substantial differences in modelled peak SWE between MEBCro_for and FSM_for are indicative of discrepancies in simulated accumulation processes. Therefore, in Fig. 7 we assess differences in the simulated canopy snow losses (c.f. Sect.

https://doi.org/10.5194/egusphere-2026-1464
Preprint. Discussion started: 22 May 2026

2.5) between the two models, which entail differences in accumulation of sub-canopy snow. Considering values averaged over all simulated WYs (Fig. 7a), canopy snow losses simulated by FSM_for are more strongly correlated with canopy density (LAI) and more variable than those simulated by MEB_for. The latter is confirmed when considering distributions of canopy snow losses for individual years (Fig. 7b), however, no clear over- or underestimation of canopy snow losses by MEBCro_for relative to FSM_for shows when considering domain-averaged values for each year. Consequently, the difference in canopy snow losses between the two models are also, albeit only weakly, correlated with LAI (Fig. 7c). MEBCro_for tends to yield higher canopy snow losses in sparse forests while FSM_for simulates larger canopy snow losses in dense forests. For grid cells with canopy density in the medium range, opposite tendencies may be observed in different years.

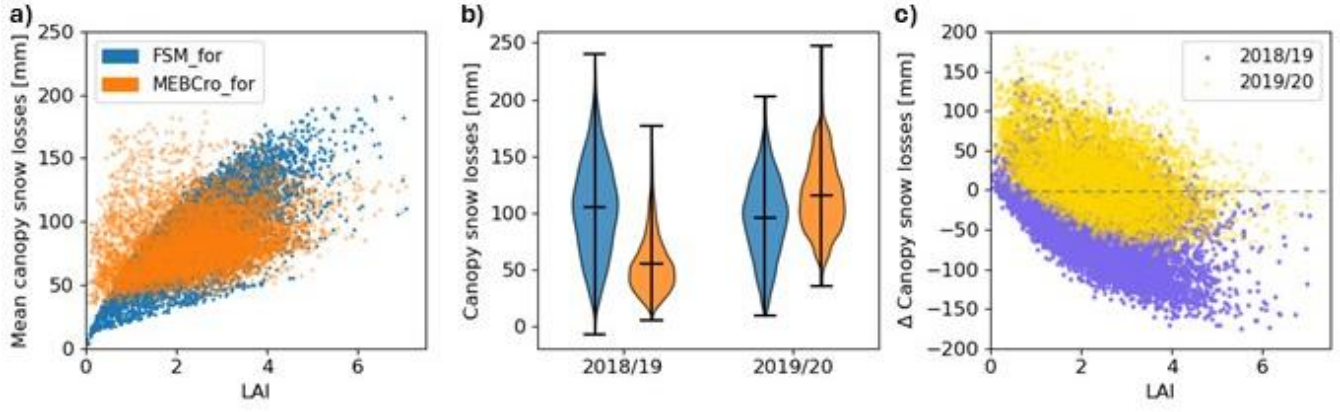

Figure 7: *Differences in canopy snow losses between MEBCro_for and FSM_for simulations averaged over all WYs and as a function of LAI (a), canopy snow loss distribution simulated by the two models for the WYs 2019 and 2020 (b), and differences in canopy snow losses between MEBCro_for and FSM_for) as a function of LAI for 2019 and 2020 (c).*

While comparing differences in modelled snow ablation processes encounters the challenges outlined in Sect. 3.2 (i.e. different ablation rates between snow schemes even in open conditions due to different treatment of snow cover fraction), the canopy has a first order impact on the amount of energy available at the snow surface through shortwave radiative transfer and longwave radiation enhancement. A comparison of sub-canopy incoming radiations is provided in Fig. 8, including average incoming long- and shortwave radiative fluxes in March, for all forested grid cells (Fig. 8a) as well as for sparse (Fig. 8b) and dense (Fig. 8c) forests separately. MEBCro_for consistently simulates stronger longwave radiation enhancement than FSM_for, with differences increasing with canopy density (28.0 W/m^2 for LAI < 2 vs. 36.5 W/m^2 for LAI > 3.5). Differences in shortwave radiation transmission exhibit a less systematic pattern. MEBCro_for allows for higher shortwave transmission than FSM_for in sparse forests (by 13 W/m^2 on average), but only for lower transmission in dense forest (-4.8 W/m^2 on average). In contrast, the homogeneous results across elevations and slope aspects suggest that topographic effects on differences in sub-canopy radiative fluxes are minor.

https://doi.org/10.5194/egusphere-2026-1464
Preprint. Discussion started: 22 May 2026

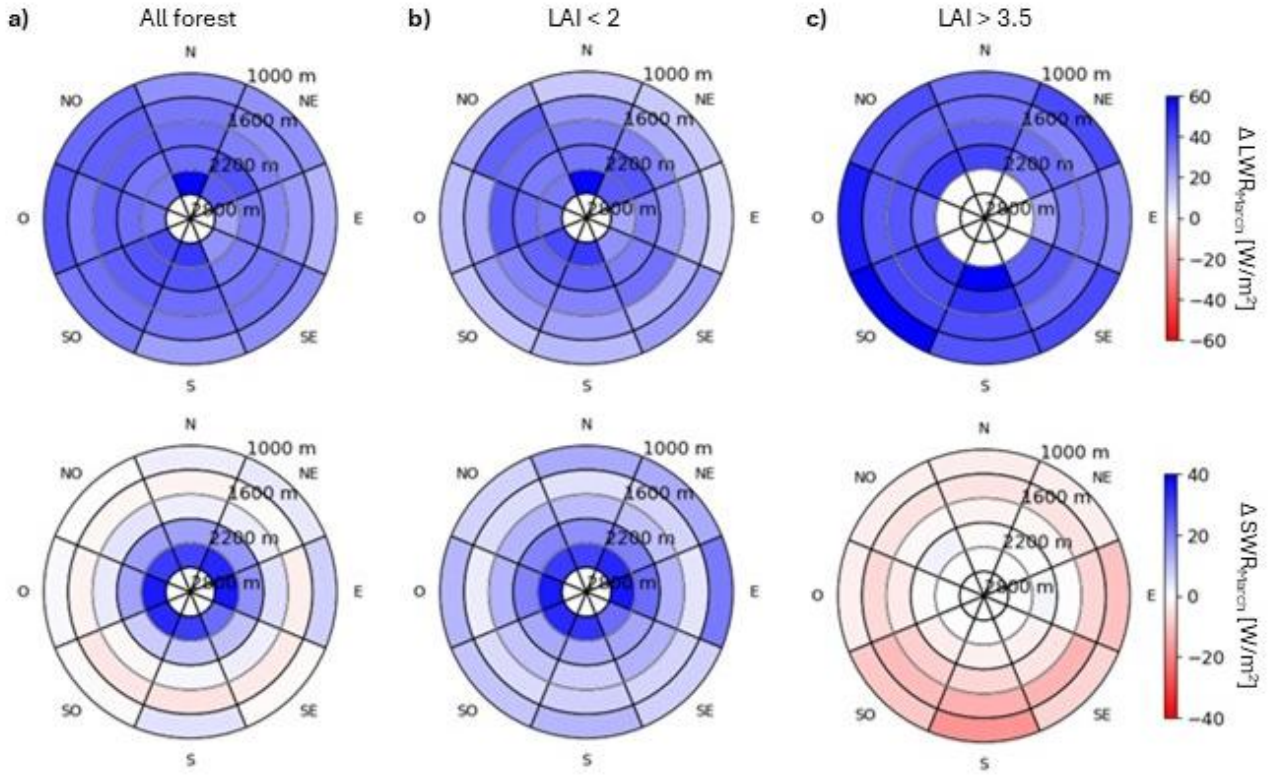

Figure 8: *Differences between subcanopy incoming longwave (upper row) and shortwave (lower row) radiation as simulated by MEB_for and FSM_for, for all forested grid cells (a) as well as for sparse (b) and dense (c) canopy separately.*

Model differences in radiative fluxes are consistent throughout the yearly cycle, as summarized in Fig. 9. Incoming longwave radiation exhibits a clear yearly cycle, which persists below the canopy for both sparse and dense forests and for both models (Fig. 9a), resulting in differences that vary within ~15 W/m^2 over the year (Fig. 9c). The same holds for shortwave radiative fluxes (Fig. 9b), however the differences between models show a more marked yearly cycle (Fig. 9c). Together, differences in short- and longwave radiative fluxes lead to a sub-canopy radiative energy input that is consistently higher for MEBCro_for than for FSM_for (Fig. 9c). Noteworthily, the overestimation of all-wave radiation by MEBCro_for is stronger for sparser canopy, because for dense canopy the stronger longwave radiation enhancement is partly compensated by reduced shortwave radiation transmissivity, especially during months with high solar angle. During winter months, differences in all-wave radiations are in the range of 30 Wm^{-2} and canopy density has only a minor impact.

https://doi.org/10.5194/egusphere-2026-1464
Preprint. Discussion started: 22 May 2026

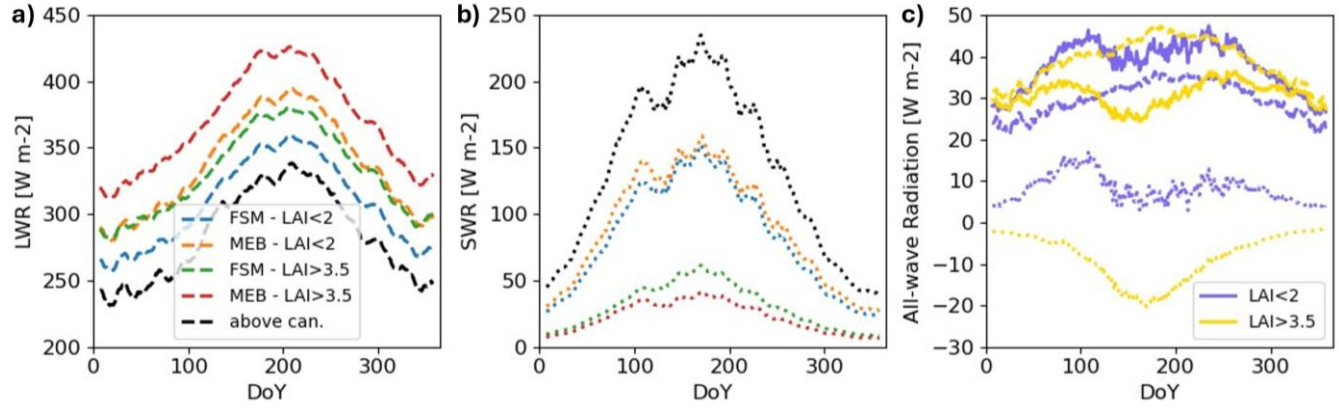

Figure 9: *Differences between sub-canopy incoming radiative fluxes throughout a yearly cycle simulated with MEB_for and FSM_for as and above the canopy, including longwave (a, dashed lines) and shortwave (b, dotted lines), as well as differences in radiative fluxes (MEB_for – FSM_for) for dense and sparse forests (c), including longwave (dashed), shortwave (dotted) and the sum of the two (full lines). All fluxes are computed as averages over the seven modelled WYs.*

3.4 Impact of a new canopy snow process parametrization in Surfex 9.0

We conclude our analysis by considering the simulation MEBCroXT_for, an update of the simulation MEBCro_for that incorporates the recent adaptations to the canopy snow process parametrizations introduced by Pauze et al. (in prep.) and based on local scale multivariate evaluations at Col de Porte, France. To this end, Fig. 10 features equivalent panels to Fig. 6, but comparing MEBCroXT_for to FSM_for. We find that the updates in MEBCroXT_for almost fully mitigate differences in peak SWE (Fig. 10a vs. 6a), which however accentuates differences in snow cover duration (Fig. 10b vs. 6b), as differences in ablation rates remain unchanged (Fig. 10c vs. 6c). Time series grouped by LAI reveal an excellent match of the SWE evolution on average. Cases where MEBCroXT_for overestimates SWE evolution only exist for dense canopies (upper quartile), however, the lower quartile of MEBCroXT_for simulations now falls below the one of FSM_for simulations for medium to dense canopies, especially in snow-poor years. Such grid cells may feature very short snow cover durations in MEBCroXT_for (see e.g. lower quartile of LAI ≥ 4.5 in 2020, Fig. 10d), which in turn entails strong underestimations of the average snow cover duration per topographic class compared to FSM_for (Fig 10b).

https://doi.org/10.5194/egusphere-2026-1464
Preprint. Discussion started: 22 May 2026

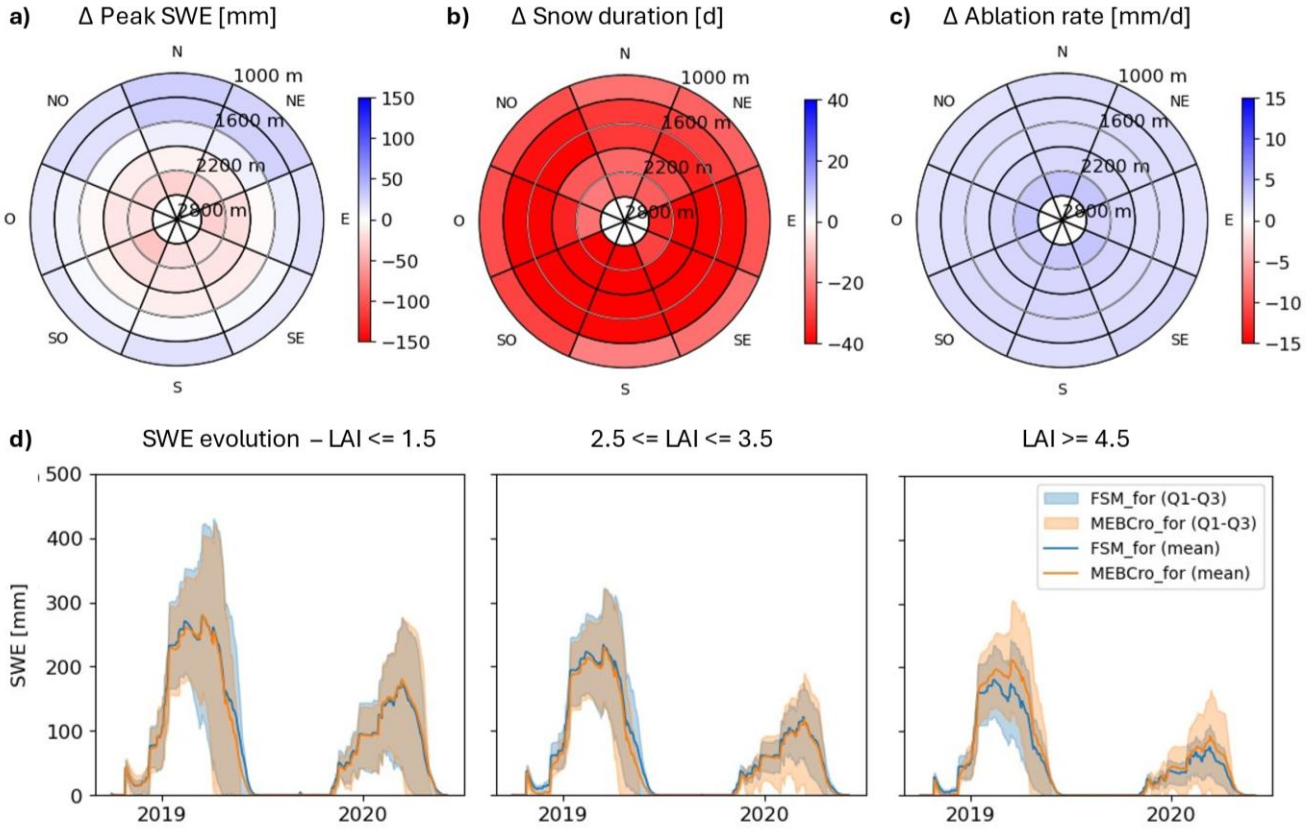

Figure 10: *Differences between MEBCroXT_for and FSM_for simulations, including peak SWE (a), snow duration (b), and ablation rate (c) aggregated by elevation band and aspect classes and averaged over the seven WYs considered. The temporal evolution of SWE differences is illustrated by SWE time series (d), with lines representing the means and shaded areas the interquartile ranges of grid cells with small (left), medium (center), and large (right) LAI values.*

As shown in Fig. 11, canopy snow losses slightly increased in MEBCroXT_for compared to MEBCro_for, on average over all WYs (Fig. 11a) as well as for individual years (Fig. 11b). As a consequence, where MEBCro_for was underestimating canopy snow losses relative to FSM_for, MEBCroTX_for now approximates them (see Fig. 11b, WY 2019), but where MEBCro_for was already overestimating canopy snow losses this positive bias is accentuated in MEBCroXT_for (see WY 2020 in Fig. 11b). Correlation of canopy snow losses to LAI remains stronger for FSM_for, and MEBCroXT_for still features higher canopy snow losses than FSM_for in sparse canopies and lower losses in dense canopies (Fig. 11c vs. Fig. 7c).

https://doi.org/10.5194/egusphere-2026-1464
Preprint. Discussion started: 22 May 2026

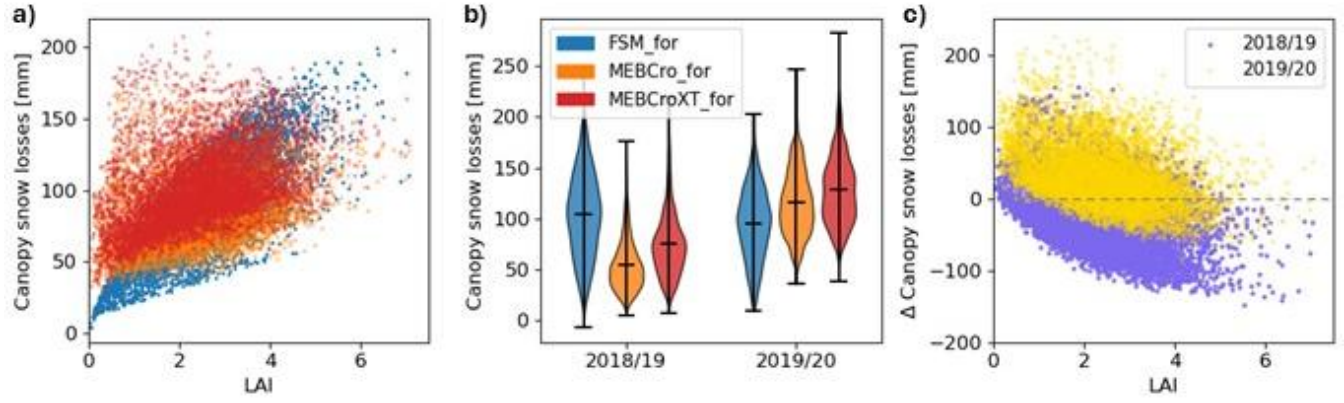

Figure 11: *Differences in canopy snow losses between MEBCroXT_for, MEBCro_for and FSM_for simulations (a) averaged over all WYs and as a function of LAI, (b) canopy snow loss distribution for the WYs 2019 and 2020, and (c) difference in canopy snow losses between MEBCroXT_for and FSM_for as a function of LAI for 2019 and 2020.*

4 Discussion

Simulations performed for this study represent the first spatially distributed application of MEB-Crocus, an indispensable step towards an operational application of the model. As traditional model evaluations focus on point-scale comparisons at flat sites, our intention in conducting a spatially distributed evaluation was to detect potential systematic biases that may be driven by canopy density, topographic setting, or specific meteorological conditions. To this end, comparison with FSM2oshd results yielded valuable insights, summarized as follows.

4.1 Structural differences pose challenges for meaningful model comparisons

Shifting from point-scale to spatially distributed model applications also implies moving from a point model to grid cells with an actual area and a specific sub-grid variability representation. These aspects introduce structural differences in the models, which give rise to additional challenges when comparing the resulting simulations. This study faced two such major challenges. Firstly, differences in the representation of sub-grid variability in land cover hampered a meaningful comparison of the default MEB-Crocus and FSM2oshd configurations. While FSM2oshd uses different tiles for forested and open grid cell fractions, MEBCro_def, when run with one single patch, uses average vegetation properties that account for both the forested and the unforested parts of a grid cell. This however leads to grid-cell-scale simulations that generally feature sparse canopies, making a process-level comparison to FSM2oshd unfeasible. A fair comparison was only possible with simulations imposing full forest cover, which still remained unfeasible with the ECOCLIMAP vegetation dataset as calculation of grid-cell scale land surface characteristics happens within SURFEX.

Second, the two models feature differences in the treatment of sub-grid variability of snow cover due to their use of different parametrizations of snow cover fraction. As shown in Sect. 3.2, this has consequences for snow cover energy input during ablation. While snow cover descriptors used in this study were computed following Mazzotti et al. (2023) and Haagmans et

https://doi.org/10.5194/egusphere-2026-1464
Preprint. Discussion started: 22 May 2026

al. (2025), the different treatment of fractional snow questions the meaningfulness of snow cover duration as a metric in this study. Snow cover mostly lasts longer in FSM2oshd, but complete snow disappearance is preceded by a phase of partial snow which is likely longer than in MEB-Crocus. Considering the impact of this structural feature on the snow ablation period, and given that models originally developed and validated at the point scale are increasingly used at gridded resolution, the treatment of fractional snow requires particular attention in future developments.

The most recent snow model intercomparison exercise, ESM-SnowMIP, highlighted numerous difficulties and pitfalls of snow model comparisons (Menard et al., 2021). They found that discrepancies in the treatment of fractional snow by different models posed issues to the evaluation of land surface albedo, yet issues related to grid cell tiling were not mentioned, although choices in the representation of surface heterogeneity are known to substantially impact snow cover simulations (Monteiro et al., 2024b).

Overall, our experience shows that such a model comparison exercise is not straightforward to set up, and that simple performance metrics may hide relevant details in identifying specific deficiencies in process representations or input data, underpinning the conclusion from Menard et al. (2021).

4.2 Vegetation datasets are a major source of model discrepancy and an avenue for model improvement

The accuracy of forest snow process representations depends on the accuracy of the chosen parametrizations, but also on the quality of the canopy structure data used to derive the canopy parameters used in these parametrizations. As noted by Rutter et al. (2009), this introduces some degree of uncertainty when applying parametrizations to new locations (and hence using new canopy data). The characterization of natural land surfaces in SURFEX with the ECOCLIMAP database is based on land cover types, which each correspond to a combination of vegetation parameters defined in lookup table, with grid-cell-scale parameters then resulting from different land cover types occupying specific fractions of that grid cell. While suitable for coarse-resolution applications, this principle is less suited to a high-resolution model system, as planned for operational use at Météo-France, where representing the actual forest structure at a specific location is more desirable.

Differences between the two default configurations of MEB-Crocus and FSM2oshd presented in Sect. 3.1 are a combination of differences in process parametrization and differences in land cover data. To isolate the relative contributions of these two sources, we consider the simulation MEBCro_all (see Sect. 2.3 and Fig. 2) as intermediate step between MEBCro_def and FSM_all. Figure 12 (upper row) presents differences in peak SWE between these three simulations. Differences between MEBCro_def and MEBCro_all (left) stem from differences in vegetation data only, while differences between MEBCro_all and FSM_all (center) stem from differences in process parametrizations alone, the two summing up to the total differences between MEBCro_def and FSM_all (right). Vegetation data and process parametrizations contribute in approximately equal amount to model discrepancies. Noteworthily, if the enhancements to the canopy snow parametrizations are taken into account (MEBCroXT_all simulation as intermediary step, lower row in Fig. 12), the contribution of process parametrizations alone decreases substantially. The time series of SWE averaged over the 1300-1900 m elevation band (lower right panel of Fig. 12) further illustrate how these four model versions relate to each other.

https://doi.org/10.5194/egusphere-2026-1464
Preprint. Discussion started: 22 May 2026

From this finding, it follows that as process parametrizations become more accurate, the quality of vegetation datasets gains importance. While seemingly obvious, this implies that switching to more detailed land cover datasets would likely entail an improvement in the performance of MEB-Crocus. As land cover datasets of increasingly high quality are becoming available (Liu et al., 2023; Marsoner et al., 2023; Webster et al., 2025), establishing a workflow to easily replace vegetation represents a fairly simple but effective avenue for model improvement. Beyond Météo-Frances future operational snow modelling system, this would benefit any spatially distributed application of MEB-Crocus by allowing easy integration of local datasets. The relevance of high-quality land surface datasets was also highlighted by Malle et al. (2024) in a study on CLM5, suggesting that enabling the use of such datasets would likely represent an improvement to other LSMs as well.

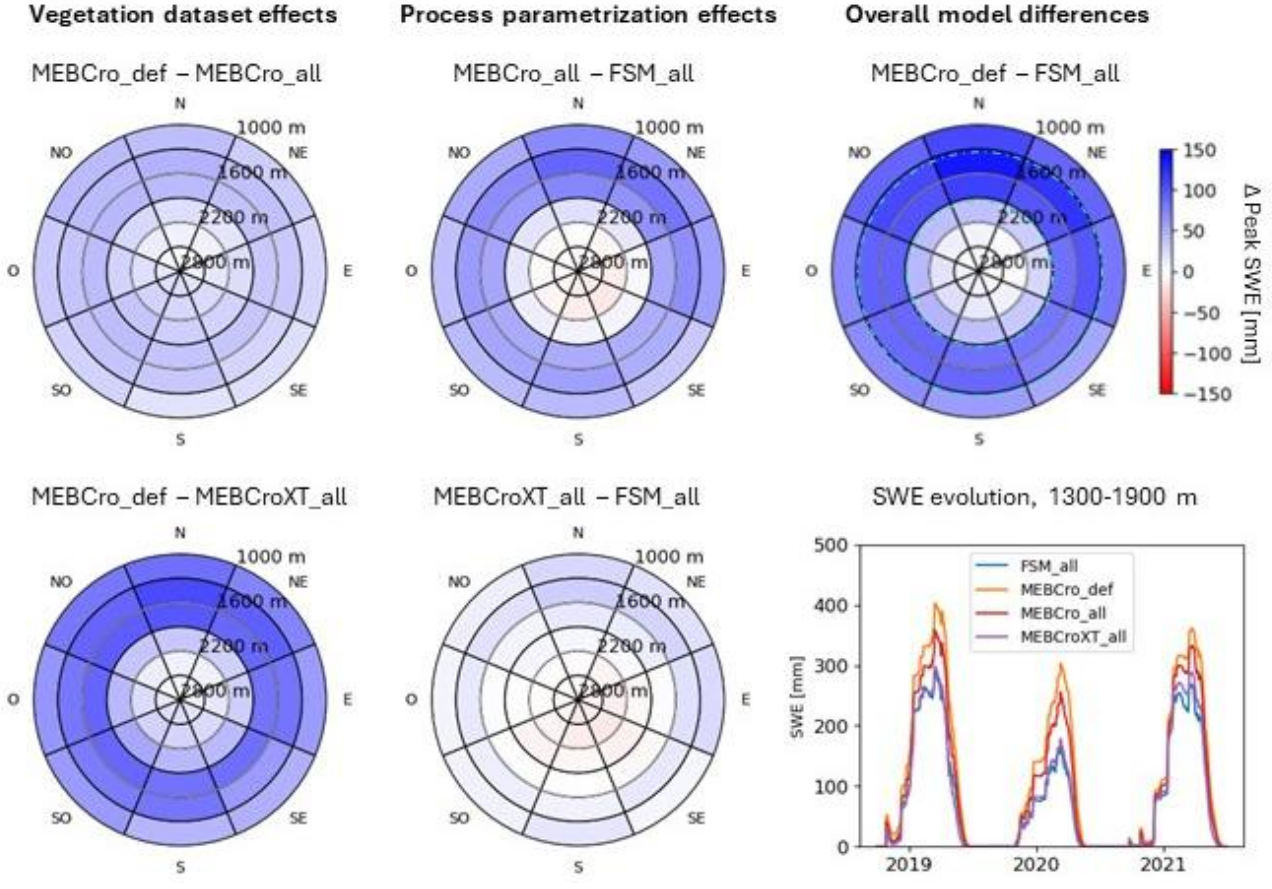

Figure 12: *Differences in peak SWE between different model configurations averaged over all WYs, and temporal evolution of SWE for the same four configurations, with lines representing the means of all grid cells in the elevation range 1300-2200m (between the two cyan dashed lines in the upper right panel).*

4.3 Canopy snow process representation outweighs topographic effects as driver of model discrepancies

Focusing on model discrepancies due to the parametrization of forest processes only (Sect. 3.3 and 3.4), our analyses revealed that generally these were more strongly linked to forest density than to topographic setting. As FSM2oshd, unlike

https://doi.org/10.5194/egusphere-2026-1464
Preprint. Discussion started: 22 May 2026

MEB-Crocus, accounts for directionality in the parametrization of shortwave radiation transfer through the canopy (Mazzotti et al., 2020b), topographically-induced patterns could in principle have been plausible. Noteworthily, the comparison of simulations without forest (Sect. 3.2) shows stronger topographic signals, but in the presence of forest these were likely confounded with forest density impacts.

Differences in canopy snow processes were found to be a major driver of differences in sub-canopy snow accumulation between MEB-Crocus and FSM2oshd, with MEB-Crocus consistently overestimating peak SWE. This finding is in agreement with observations from Vincent et al. (2018), who identified interception as the main reason of model bias in their site-scale evaluation. Recent changes to the representation of snow interception by the canopy and its subsequent unloading largely eliminated these differences, however, differences in canopy snow losses persisted. This suggests that the smaller peak SWE bias achieved by MEBCroXT_for is not only a consequence of increased canopy snow sublimation, but also of higher early-season melt, likely induced by updates in the properties of snow unloading and melt drip from the canopy. As commented by Lundquist et al. (2021), assessing and improving parametrizations of this process remains difficult (Lumbrazo et al., 2022). Recent attempts to explicitly compute the energy balance of intercepted snow might provide a way forward (Cebulski and Pomeroy, 2026), but also raise numerical challenges in the coupling between components (Lafaysse et al., 2025).

Analysis of sub-canopy radiation showed that energy inputs to the forest snowpacks are larger for MEB-Crocus than for FSM2oshd, which is mainly due to stronger longwave radiation enhancement, especially for dense canopies. During the melt period, when the snowpack is frequently isothermal, differences in incoming longwave radiation translate directly into differences in net longwave radiation input. Differences in net shortwave radiation input, on the contrary, are further determined by potential differences in snow albedo. Both FSM2oshd and MEB-Crocus were found to accurately reproduce sub-canopy longwave radiation observations at the point scale (Mazzotti et al., 2020b; Vincent et al., 2018), albeit at different sites, and, in the case of MEB-Crocus, for a limited number of points and LAI range. This apparent contradiction to our findings might be explained the limited extent of the MEB-Crocus evaluation, but also by differences in the approaches used to derive canopy structure characteristics at the sites used for these two evaluations: in-situ methods to derive LAI are many, and sometimes yield diverging results (Jonckheere et al., 2004). More in-depth investigations would be required to establish if overestimation of longwave radiation enhancement is due to an overestimation of canopy temperature, or rather to the parametrization of the longwave radiation emission from the canopy as a function of LAI.

4.4 Model comparison studies are instructive despite inherent limitations

Although much effort has been put into validating the forest snow scheme implemented into FSM2oshd (see Sect. 2.2), it must be kept in mind that it remains a model which cannot fully replace ground truth. Unarguably, continued efforts to obtain experimental data on forest-snow processes remain valuable. Instead, assessment against a benchmark model should rather be seen as a complementary undertaking which also holds some advantages. First, process-based modelling yields spatiotemporally continuous information for a set of state variables and fluxes that no assessment based on real-world data

https://doi.org/10.5194/egusphere-2026-1464
Preprint. Discussion started: 22 May 2026

can provide. Indeed, even LiDAR-based spatial observations of forest snow provide at best snow depth maps for a few dates, in most cases for small areas only (e.g. Geissler et al. (2025); Ylönen et al. (2025)). Moreover, simulations spanning multiple winters allow assessing the impact of varying meteorological conditions, which has been shown to alter forest snow dynamics (Bouchard et al., 2024a). While our findings were generally consistent between years, low-snow winters were associated with stronger model discrepancies for both simulations with forest (Fig. 10d) and without (Fig. 5d). Mid-winter melt events are a known challenge for physics-based snow models (Cristea et al., 2022), but expected to become more frequent in a warming climate (López-Moreno et al., 2024), especially at elevations typical of sub-alpine forests (Matiu et al., 2021), which is why considering such conditions in model evaluations is increasingly important.

A disadvantage of using FSM2oshd as benchmark model specifically was the limitation of our analysis to SWE and radiation fluxes below canopy, since evolution of snow microstructure is not included in the model. The large structural differences in snowpack representations between the two models, with FSM2oshd being less detailed, was part of our motivation to focus on the analyses on processes that are solely influenced by canopy. A full evaluation of model discrepancies would have required analyzing all energy fluxes to/from the snowpack, which was however out of scope here.

Despite these inherent methodological limitations, the model comparisons conducted in this study shed light on some existing challenges and potential avenues for continued development of MEB-Crocus, highlighting the interest of a spatially distributed model evaluation across a broad range of topographic settings, forest structures, and meteorological conditions.

5. Conclusion

For the first time, this study presented fully distributed forest snow simulations obtained with the MEB-Crocus scheme within the SURFEX land surface modelling platform over a topographically complex and partially forested domain in the European Alps, and attempted a spatially explicit evaluation of these simulations through targeted comparison to FSM2oshd, considered as a benchmark model. This work thus constitutes an important step in view of the model's upcoming usage in Météo-France's operational snow modelling chain. A suite of model experiments using MEB-Crocus in different configurations and assessment against FSM2oshd revealed substantial differences between the default versions of the two models, with MEB-Crocus generally yielding larger peak SWE than FSM2oshd, although snow duration was longer fore FSM2oshd at high elevations. Yet, structural differences between the two models hampered attribution of these differences to specific model parameters or processes. Only additional targeted model experiments allowed unraveling the origin of these model discrepancies.

Assessing the relative contribution of land cover datasets and process parametrization highlighted the importance of detailed land cover data. When identical land surface information was used by both models, discrepancies were found to be more strongly dependent on forest density than on topographic setting. Differences in canopy snow process parametrizations led to MEB-Crocus generally overestimating peak SWE, especially for denser canopies. Discrepancies in peak SWE were largely mitigated by recent updates to the parametrizations of snow interception by and unloading from the canopy, however

https://doi.org/10.5194/egusphere-2026-1464
Preprint. Discussion started: 22 May 2026

differences in canopy snow losses persisted. MEB-Crocus consistently overestimated sub-canopy incoming longwave radiation, especially for dense canopies, while shortwave radiation was only overestimated for sparse canopies but rather underestimated for dense canopies. Results were largely consistent between years. While these model experiments highlighted the difficulties associated with making such model experiments meaningful, they also yielded valuable insights that should encourage similar evaluation exercises in the future. Capitalizing on previous evaluations of a well-established snow-vegetation model, models intercomparison give access to extended spatio-temporal analyses of the behavior or new models and included processes in the context of still challenging direct observation of the spatial variability of snow under forest.

Code and data availability

MEB-Crocus runs rely on the SURFEX platform, accessible as described at https://github.com/UMR-CNRM/snowtools/blob/master/doc/source/misc/surfex-install.rst (last access: 10 March 2026). The version used in this work is tagged as Mazzotti_2026. The corresponding code, settings, and land surface input files are available under: https://zenodo.org/uploads/18888458. FSM2oshd runs correspond to those presented by Haagmans et al. (2025), with corresponding code available under DOI: 10.5281/zenodo.14290599.

Acknowledgements

GM acknowledges funding from the Swiss National Science Foundation, grants P500PN_202741 and P5R5PN_225378. Internships of FV and AC were funded by the Région Auvergne-Rhone-Alpes through the project SENSASS. JPN received funding from the Research Council of Finland (grant 356138). We are grateful to Aaron Boone for his help with MEB, to Yves Lejeune, Axel Bouchet and Thomas Pauze from CEN for their work on canopy snow processes, and to Tobias Jonas, Louis Quéno and Bertrand Cluzet from the OSHD team at SLF for insightful discussions and their support of this project. IGE and CNRM/CEN are part of LabEX OSUG@2020.

Author contributions

GM, ML and IG conceived and supervised the study.
FV, AC and GM performed the analyses, with input from JPN, IG, ML.
MF and JM ran and managed the MEB-Crocus and FSM2oshd simulations, respectively.
GM wrote the manuscript, with inputs and feedback from all coauthors.

https://doi.org/10.5194/egusphere-2026-1464
Preprint. Discussion started: 22 May 2026

References

Avanzi, F., Gabellani, S., Delogu, F., Silvestro, F., Pignone, F., Bruno, G., Pulvirenti, L., Squicciarino, G., Fiori, E., Rossi, L., Puca, S., Toniazzo, A., Giordano, P., Falzacappa, M., Ratto, S., Stevenin, H., Cardillo, A., Fioletti, M., Cazzuli, O., Cremonese, E., Morra di Cella, U., Ferraris, L., 2023. IT-SNOW: a snow reanalysis for Italy blending modeling, in situ data, and satellite observations (2010–2021). Earth Syst. Sci. Data 15, 639–660. https://doi.org/10.5194/essd-15-639-2023

Barnhart, T.B., Putman, A.L., Heldmyer, A.J., Rey, D.M., Hammond, J.C., Driscoll, J.M., Sexstone, G.A., 2024. Evaluating Distributed Snow Model Resolution and Meteorology Parameterizations Against Streamflow Observations: Finer Is Not Always Better. Water Resour. Res. 60, e2023WR035982. https://doi.org/10.1029/2023WR035982

Bartelt, P., Lehning, M., 2002. A physical SNOWPACK model for the Swiss avalanche warning: Part I: numerical model. Cold Reg. Sci. Technol. 35, 123–145. https://doi.org/10.1016/S0165-232X(02)00074-5

Berg, J., Reynolds, D., Quéno, L., Jonas, T., Lehning, M., Mott, R., 2024. A seasonal snowpack model forced with dynamically downscaled forcing data resolves hydrologically relevant accumulation patterns. Front. Earth Sci. 12. https://doi.org/10.3389/feart.2024.1393260

Bonner, H.M., Smyth, E., Raleigh, M.S., Small, E.E., 2022. A Meteorology and Snow Data Set From Adjacent Forested and Meadow Sites at Crested Butte, CO, USA. Water Resour. Res. 58, e2022WR033006. https://doi.org/10.1029/2022WR033006

Boone, A., Samuelsson, P., Gollvik, S., Napoly, A., Jarlan, L., Brun, E., Decharme, B., 2017. The interactions between soil–biosphere–atmosphere land surface model with a multi-energy balance (ISBA-MEB) option in SURFEXv8 – Part 1: Model description. Geosci. Model Dev. 10, 843–872. https://doi.org/10.5194/gmd-10-843-2017

Bouchard, B., Nadeau, D.F., Domine, F., Anctil, F., Jonas, T., Tremblay, É., 2024a. How does a warm and low-snow winter impact the snow cover dynamics in a humid and discontinuous boreal forest? Insights from observations and modeling in eastern Canada. Hydrol. Earth Syst. Sci. 28, 2745–2765. https://doi.org/10.5194/hess-28-2745-2024

Bouchard, B., Nadeau, D.F., Domine, F., Wever, N., Michel, A., Lehning, M., Isabelle, P.-E., 2024b. Impact of intercepted and sub-canopy snow microstructure on snowpack response to rain-on-snow events under a boreal canopy. The Cryosphere 18, 2783–2807. https://doi.org/10.5194/tc-18-2783-2024

Broxton, P.D., Moeser, C.D., Harpold, A., 2021. Accounting for Fine-Scale Forest Structure is Necessary to Model Snowpack Mass and Energy Budgets in Montane Forests. Water Resour. Res. 57, e2021WR029716. https://doi.org/10.1029/2021WR029716

Brun, E., David, P., Sudul, M., Brunot, G., 1992. A numerical model to simulate snow-cover stratigraphy for operational avalanche forecasting. J. Glaciol. 38, 13–22. https://doi.org/10.3189/S0022143000009552

Cebulski, A.C., Pomeroy, J.W., 2026. Processes Governing the Ablation of Intercepted Snow. Water Resour. Res. 62, e2025WR042009. https://doi.org/10.1029/2025WR042009

https://doi.org/10.5194/egusphere-2026-1464
Preprint. Discussion started: 22 May 2026

Clark, M.P., Hendrikx, J., Slater, A.G., Kavetski, D., Anderson, B., Cullen, N.J., Kerr, T., Örn Hreinsson, E., Woods, R.A., 2011. Representing spatial variability of snow water equivalent in hydrologic and land-surface models: A review. Water Resour. Res. 47. https://doi.org/10.1029/2011WR010745

Cluzet, B., Magnusson, J., Quéno, L., Mazzotti, G., Mott, R., Jonas, T., 2024. Exploring how Sentinel-1 wet-snow maps can inform fully distributed physically based snowpack models. The Cryosphere 18, 5753–5767. https://doi.org/10.5194/tc-18-5753-2024

Cristea, N.C., Bennett, A., Nijssen, B., Lundquist, J.D., 2022. When and Where Are Multiple Snow Layers Important for Simulations of Snow Accumulation and Melt? Water Resour. Res. 58, e2020WR028993. https://doi.org/10.1029/2020WR028993

Currier, W., Pflug, J., Mazzotti, G., Jonas, T., Deems, J., Bormann, K., Painter, T., Hiemstra, C., Gelvin, A., Uhlmann, Z., Spaete, L., Glenn, N., Lundquist, J., 2019. Comparing Aerial Lidar Observations With Terrestrial Lidar and Snow-Probe Transects From NASA's 2017 SnowEx Campaign. Water Resour. Res. 55. https://doi.org/10.1029/2018WR024533

Decharme, B., Brun, E., Boone, A., Delire, C., Le Moigne, P., Morin, S., 2016. Impacts of snow and organic soils parameterization on northern Eurasian soil temperature profiles simulated by the ISBA land surface model. The Cryosphere 10, 853–877. https://doi.org/10.5194/tc-10-853-2016

Deschamps-Berger, C., Gascoin, S., Shean, D., Besso, H., Guiot, A., López-Moreno, J.I., 2023. Evaluation of snow depth retrievals from ICESat-2 using airborne laser-scanning data. The Cryosphere 17, 2779–2792. https://doi.org/10.5194/tc-17-2779-2023

Deschamps-Berger, C., López-Moreno, J.I., Gascoin, S., Mazzotti, G., Boone, A., 2025. Where Snow and Forest Meet: A Global Atlas. Geophys. Res. Lett. 52, e2024GL113684. https://doi.org/10.1029/2024GL113684

Essery, R., 2015. A factorial snowpack model (FSM 1.0). Geosci. Model Dev. 8, 3867–3876. https://doi.org/10.5194/gmd-8-3867-2015

Essery, R., Mazzotti, G., Barr, S., Jonas, T., Quaife, T., Rutter, N., 2025. A Flexible Snow Model (FSM 2.1.1) including a forest canopy. Geosci. Model Dev. 18, 3583–3605. https://doi.org/10.5194/gmd-18-3583-2025

Essery, R., Pomeroy, J., 2004. Implications of spatial distributions of snow mass and melt rate for snow-cover depletion: theoretical considerations. Ann. Glaciol. 38, 261–265. https://doi.org/10.3189/172756404781815275

Essery, R., Rutter, N., Pomeroy, J., Baxter, R., Stähli, M., Gustafsson, D., Barr, A., Bartlett, P., Elder, K., 2009. SNOWMIP2: An Evaluation of Forest Snow Process Simulations. Bull. Am. Meteorol. Soc. 90, 1120–1136. https://doi.org/10.1175/2009BAMS2629.1

Faroux, S., Kaptué Tchuenté, A.T., Roujean, J.-L., Masson, V., Martin, E., Le Moigne, P., 2013. ECOCLIMAP-II/Europe: a twofold database of ecosystems and surface parameters at 1 km resolution based on satellite information for use in land surface, meteorological and climate models. Geosci. Model Dev. 6, 563–582. https://doi.org/10.5194/gmd-6-563-2013

https://doi.org/10.5194/egusphere-2026-1464
Preprint. Discussion started: 22 May 2026

Förster, K., Garvelmann, J., Meißl, G., Strasser, U., 2018. Modelling forest snow processes with a new version of WaSiM. Hydrol. Sci. J. 63, 1540–1557. https://doi.org/10.1080/02626667.2018.1518626

Gascoin, S., Grizonnet, M., Bouchet, M., Salgues, G., Hagolle, O., 2019. Theia Snow collection: high-resolution operational snow cover maps from Sentinel-2 and Landsat-8 data. Earth Syst. Sci. Data 11, 493–514. https://doi.org/10.5194/essd-11-493-2019

Gascoin, S., Luojus, K., Nagler, T., Lievens, H., Masiokas, M., Jonas, T., Zheng, Z., De Rosnay, P., 2024. Remote sensing of mountain snow from space: status and recommendations. Front. Earth Sci. 12. https://doi.org/10.3389/feart.2024.1381323

Geissler, J., Mazzotti, G., Rathmann, L., Webster, C., Weiler, M., 2025. Forest Snow Patterns Derived Using ClustSnow Are Temporally Persistent Under Variable Environmental Conditions. Water Resour. Res. 61, e2024WR038442. https://doi.org/10.1029/2024WR038442

Haagmans, V., Mazzotti, G., Webster, C., Jonas, T., 2025. How montane forests shape snow cover dynamics across the central European Alps. EGUsphere 1–29. https://doi.org/10.5194/egusphere-2025-3843

Haddjeri, A., Baron, M., Lafaysse, M., Le Toumelin, L., Deschamps-Berger, C., Vionnet, V., Gascoin, S., Vernay, M., Dumont, M., 2024. Analyzing the sensitivity of a blowing snow model (SnowPappus) to precipitation forcing, blowing snow, and spatial resolution. The Cryosphere 18, 3081–3116. https://doi.org/10.5194/tc-18-3081-2024

He, C., Valayamkunnath, P., Barlage, M., Chen, F., Gochis, D., Cabell, R., Schneider, T., Rasmussen, R., Niu, G.-Y., Yang, Z.-L., Niyogi, D., Ek, M., 2023. Modernizing the open-source community Noah with multi-parameterization options (Noah-MP) land surface model (version 5.0) with enhanced modularity, interoperability, and applicability. Geosci. Model Dev. 16, 5131–5151. https://doi.org/10.5194/gmd-16-5131-2023

Hou, Y., Yang, Y., Han, J., Woods, R., Yan, Z., 2025. Impacts of snow changes on hydropower potential under a changing climate. J. Hydrol. 661, 133747. https://doi.org/10.1016/j.jhydrol.2025.133747

Jonckheere, I., Fleck, S., Nackaerts, K., Muys, B., Coppin, P., Weiss, M., Baret, F., 2004. Review of methods for in situ leaf area index determination: Part I. Theories, sensors and hemispherical photography. Agric. For. Meteorol. 121, 19–35. https://doi.org/10.1016/j.agrformet.2003.08.027

Kneib, M., Dehecq, A., Gilbert, A., Basset, A., Miles, E., Jouvet, G., Jourdain, B., Ducasse, E., Béraud, L., Rabatel, A., Mouginot, J., Carcanade, G., Laarman, O., Brun, F., Six, D., 2024. Distributed surface mass balance of an avalanche-fed glacier. The Cryosphere 18, 5965–5983. https://doi.org/10.5194/tc-18-5965-2024

Kraft, M., McNamara, J.P., Marshall, H.-P., Glenn, N.F., 2022. Forest impacts on snow accumulation and melt in a semi-arid mountain environment. Front. Water 4. https://doi.org/10.3389/frwa.2022.1004123

Krinner, G., Derksen, C., Essery, R., Flanner, M., Hagemann, S., Clark, M., Hall, A., Rott, H., Brutel-Vuilmet, C., Kim, H., Ménard, C.B., Mudryk, L., Thackeray, C., Wang, L., Arduini, G., Balsamo, G., Bartlett, P., Boike, J., Boone, A., Chéruy,

https://doi.org/10.5194/egusphere-2026-1464
Preprint. Discussion started: 22 May 2026

F., Colin, J., Cuntz, M., Dai, Y., Decharme, B., Derry, J., Ducharne, A., Dutra, E., Fang, X., Fierz, C., Ghattas, J., Gusev, Y., Haverd, V., Kontu, A., Lafaysse, M., Law, R., Lawrence, D., Li, W., Marke, T., Marks, D., Ménégoz, M., Nasonova, O., Nitta, T., Niwano, M., Pomeroy, J., Raleigh, M.S., Schaedler, G., Semenov, V., Smirnova, T.G., Stacke, T., Strasser, U., Svenson, S., Turkov, D., Wang, T., Wever, N., Yuan, H., Zhou, W., Zhu, D., 2018. ESM-SnowMIP: assessing snow models and quantifying snow-related climate feedbacks. Geosci. Model Dev. 11, 5027–5049. https://doi.org/10.5194/gmd-11-5027-2018

Lafaysse, M., Dumont, M., De Fleurian, B., Fructus, M., Nheili, R., Viallon-Galinier, L., Baron, M., Boone, A., Bouchet, A., Brondex, J., Carmagnola, C., Cluzet, B., Fourteau, K., Haddjeri, A., Hagenmuller, P., Mazzotti, G., Minvielle, M., Morin, S., Quéno, L., Roussel, L., Spandre, P., Tuzet, F., Vionnet, V., 2025. Version 3.0 of the Crocus snowpack model. EGUsphere 1–75. https://doi.org/10.5194/egusphere-2025-4540

Lawrence, D.M., Fisher, R.A., Koven, C.D., Oleson, K.W., Swenson, S.C., Bonan, G., Collier, N., Ghimire, B., van Kampenhout, L., Kennedy, D., Kluzek, E., Lawrence, P.J., Li, F., Li, H., Lombardozzi, D., Riley, W.J., Sacks, W.J., Shi, M., Vertenstein, M., Wieder, W.R., Xu, C., Ali, A.A., Badger, A.M., Bisht, G., van den Broeke, M., Brunke, M.A., Burns, S.P., Buzan, J., Clark, M., Craig, A., Dahlin, K., Drewniak, B., Fisher, J.B., Flanner, M., Fox, A.M., Gentine, P., Hoffman, F., Keppel-Aleks, G., Knox, R., Kumar, S., Lenaerts, J., Leung, L.R., Lipscomb, W.H., Lu, Y., Pandey, A., Pelletier, J.D., Perket, J., Randerson, J.T., Ricciuto, D.M., Sanderson, B.M., Slater, A., Subin, Z.M., Tang, J., Thomas, R.Q., Val Martin, M., Zeng, X., 2019. The Community Land Model Version 5: Description of New Features, Benchmarking, and Impact of Forcing Uncertainty. J. Adv. Model. Earth Syst. 11, 4245–4287. https://doi.org/10.1029/2018MS001583

Le Roux, E., Evin, G., Samacoïts, R., Eckert, N., Blanchet, J., Morin, S., 2023. Projection of snowfall extremes in the French Alps as a function of elevation and global warming level. The Cryosphere 17, 4691–4704. https://doi.org/10.5194/tc-17-4691-2023

Liu, S., Brandt, M., Nord-Larsen, T., Chave, J., Reiner, F., Lang, N., Tong, X., Ciais, P., Igel, C., Pascual, A., Guerra-Hernandez, J., Li, S., Mugabowindekwe, M., Saatchi, S., Yue, Y., Chen, Z., Fensholt, R., 2023. The overlooked contribution of trees outside forests to tree cover and woody biomass across Europe. Sci. Adv. 9, eadh4097. https://doi.org/10.1126/sciadv.adh4097

López-Moreno, J.I., Callow, N., McGowan, H., Webb, R., Schwartz, A., Bilish, S., Revuelto, J., Gascoin, S., Deschamps-Berger, C., Alonso-González, E., 2024. Marginal snowpacks: The basis for a global definition and existing research needs. Earth-Sci. Rev. 252, 104751. https://doi.org/10.1016/j.earscirev.2024.104751

Lumbrazo, C., Bennett, A., Currier, W.R., Nijssen, B., Lundquist, J., 2022. Evaluating Multiple Canopy-Snow Unloading Parameterizations in SUMMA With Time-Lapse Photography Characterized by Citizen Scientists. Water Resour. Res. 58, e2021WR030852. https://doi.org/10.1029/2021WR030852

https://doi.org/10.5194/egusphere-2026-1464
Preprint. Discussion started: 22 May 2026

Lundquist, J.D., Dickerson-Lange, S., Gutmann, E., Jonas, T., Lumbrazo, C., Reynolds, D., 2021. Snow interception modelling: Isolated observations have led to many land surface models lacking appropriate temperature sensitivities. Hydrol. Process. 35, e14274. https://doi.org/10.1002/hyp.14274

Lute, A.C., Abatzoglou, J., Link, T., 2022. SnowClim v1.0: high-resolution snow model and data for the western United States. Geosci. Model Dev. 15, 5045–5071. https://doi.org/10.5194/gmd-15-5045-2022

Magnusson, J., Gustafsson, D., Hüsler, F., Jonas, T., 2014. Assimilation of point SWE data into a distributed snow cover model comparing two contrasting methods. Water Resour. Res. 50, 7816–7835. https://doi.org/10.1002/2014WR015302

Malle, J.T., Mazzotti, G., Karger, D.N., Jonas, T., 2024. Regionally optimized high-resolution input datasets enhance the representation of snow cover in CLM5. Earth Syst. Dyn. 15, 1073–1115. https://doi.org/10.5194/esd-15-1073-2024

Marsh, C.B., Pomeroy, J.W., Wheater, H.S., 2020. The Canadian Hydrological Model (CHM) v1.0: a multi-scale, multi-extent, variable-complexity hydrological model – design and overview. Geosci. Model Dev. 13, 225–247. https://doi.org/10.5194/gmd-13-225-2020

Marsoner, T., Simion, H., Giombini, V., Egarter Vigl, L., Candiago, S., 2023. A detailed land use/land cover map for the European Alps macro region. Sci. Data 10, 468. https://doi.org/10.1038/s41597-023-02344-3

Matiu, M., Crespi, A., Bertoldi, G., Carmagnola, C.M., Marty, C., Morin, S., Schöner, W., Cat Berro, D., Chiogna, G., De Gregorio, L., Kotlarski, S., Majone, B., Resch, G., Terzago, S., Valt, M., Beozzo, W., Cianfarra, P., Gouttevin, I., Marcolini, G., Notarnicola, C., Petitta, M., Scherrer, S.C., Strasser, U., Winkler, M., Zebisch, M., Cicogna, A., Cremonini, R., Debernardi, A., Faletto, M., Gaddo, M., Giovannini, L., Mercalli, L., Soubeyroux, J.-M., Sušnik, A., Trenti, A., Urbani, S., Weilguni, V., 2021. Observed snow depth trends in the European Alps: 1971 to 2019. The Cryosphere 15, 1343–1382. https://doi.org/10.5194/tc-15-1343-2021

Mazzotti, G., Essery, R., Moeser, C.D., Jonas, T., 2020a. Resolving Small-Scale Forest Snow Patterns Using an Energy Balance Snow Model With a One-Layer Canopy. Water Resour. Res. 56, e2019WR026129. https://doi.org/10.1029/2019WR026129

Mazzotti, G., Essery, R., Webster, C., Malle, J., Jonas, T., 2020b. Process-Level Evaluation of a Hyper-Resolution Forest Snow Model Using Distributed Multisensor Observations. Water Resour. Res. 56, e2020WR027572. https://doi.org/10.1029/2020WR027572

Mazzotti, G., Webster, C., Essery, R., Jonas, T., 2021. Increasing the Physical Representation of Forest-Snow Processes in Coarse-Resolution Models: Lessons Learned From Upscaling Hyper-Resolution Simulations. Water Resour. Res. 57, e2020WR029064. https://doi.org/10.1029/2020WR029064

Mazzotti, G., Webster, C., Quéno, L., Cluzet, B., Jonas, T., 2023. Canopy structure, topography, and weather are equally important drivers of small-scale snow cover dynamics in sub-alpine forests. Hydrol. Earth Syst. Sci. 27, 2099–2121. https://doi.org/10.5194/hess-27-2099-2023

https://doi.org/10.5194/egusphere-2026-1464
Preprint. Discussion started: 22 May 2026

Menard, C.B., Essery, R., Krinner, G., Arduini, G., Bartlett, P., Boone, A., Brutel-Vuilmet, C., Burke, E., Cuntz, M., Dai, Y., Decharme, B., Dutra, E., Fang, X., Fierz, C., Gusev, Y., Hagemann, S., Haverd, V., Kim, H., Lafaysse, M., Marke, T., Nasonova, O., Nitta, T., Niwano, M., Pomeroy, J., Schädler, G., Semenov, V.A., Smirnova, T., Strasser, U., Swenson, S., Turkov, D., Wever, N., Yuan, H., 2021. Scientific and Human Errors in a Snow Model Intercomparison. Bull. Am. Meteorol. Soc. 102, E61–E79. https://doi.org/10.1175/BAMS-D-19-0329.1

Michalet, R., Touzard, B., Billard, G., Choler, P., Loucougaray, G., 2024. Changes in taxonomic and functional composition of subalpine plant communities in response to climate change under contrasting conditions of bedrock and snow cover duration. J. Veg. Sci. 35, e13253. https://doi.org/10.1111/jvs.13253

Monteiro, D., Caillaud, C., Lafaysse, M., Napoly, A., Fructus, M., Alias, A., Morin, S., 2024a. Improvements in the land surface configuration to better simulate seasonal snow cover in the European Alps with the CNRM-AROME (cycle 46) convection-permitting regional climate model. Geosci. Model Dev. 17, 7645–7677. https://doi.org/10.5194/gmd-17-7645-2024

Monteiro, D., Caillaud, C., Lafaysse, M., Napoly, A., Fructus, M., Alias, A., Morin, S., 2024b. Improvements in the land surface configuration to better simulate seasonal snow cover in the European Alps with the CNRM-AROME (cycle 46) convection-permitting regional climate model. Geosci. Model Dev. 17, 7645–7677. https://doi.org/10.5194/gmd-17-7645-2024

Morin, S., Horton, S., Techel, F., Bavay, M., Coléou, C., Fierz, C., Gobiet, A., Hagenmuller, P., Lafaysse, M., Ližar, M., Mitterer, C., Monti, F., Müller, K., Olefs, M., Snook, J.S., van Herwijnen, A., Vionnet, V., 2020. Application of physical snowpack models in support of operational avalanche hazard forecasting: A status report on current implementations and prospects for the future. Cold Reg. Sci. Technol. 170, 102910. https://doi.org/10.1016/j.coldregions.2019.102910

Mott, R., Winstral, A., Cluzet, B., Helbig, N., Magnusson, J., Mazzotti, G., Quéno, L., Schirmer, M., Webster, C., Jonas, T., 2023. Operational snow-hydrological modeling for Switzerland. Front. Earth Sci. 11. https://doi.org/10.3389/feart.2023.1228158

Napoly, A., Boone, A., Welfringer, T., 2020. ISBA-MEB (SURFEX v8.1): model snow evaluation for local-scale forest sites. Geosci. Model Dev. 13, 6523–6545. https://doi.org/10.5194/gmd-13-6523-2020

Notarnicola, C., 2020. Hotspots of snow cover changes in global mountain regions over 2000–2018. Remote Sens. Environ. 243, 111781. https://doi.org/10.1016/j.rse.2020.111781

Nousu, J.-P., Lafaysse, M., Mazzotti, G., Ala-aho, P., Marttila, H., Cluzet, B., Aurela, M., Lohila, A., Kolari, P., Boone, A., Fructus, M., Launiainen, S., 2024. Modeling snowpack dynamics and surface energy budget in boreal and subarctic peatlands and forests. The Cryosphere 18, 231–263. https://doi.org/10.5194/tc-18-231-2024

https://doi.org/10.5194/egusphere-2026-1464
Preprint. Discussion started: 22 May 2026

Olefs, M., Koch, R., Schöner, W., Marke, T., 2020. Changes in Snow Depth, Snow Cover Duration, and Potential Snowmaking Conditions in Austria, 1961–2020—A Model Based Approach. Atmosphere 11, 1330. https://doi.org/10.3390/atmos11121330

Painter, T.H., Berisford, D.F., Boardman, J.W., Bormann, K.J., Deems, J.S., Gehrke, F., Hedrick, A., Joyce, M., Laidlaw, R., Marks, D., Mattmann, C., McGurk, B., Ramirez, P., Richardson, M., Skiles, S.M., Seidel, F.C., Winstral, A., 2016. The Airborne Snow Observatory: Fusion of scanning lidar, imaging spectrometer, and physically-based modeling for mapping snow water equivalent and snow albedo. Remote Sens. Environ. 184, 139–152. https://doi.org/10.1016/j.rse.2016.06.018

Quéno, L., Mott, R., Morin, P., Cluzet, B., Mazzotti, G., Jonas, T., 2024. Snow redistribution in an intermediate-complexity snow hydrology modelling framework. The Cryosphere 18, 3533–3557. https://doi.org/10.5194/tc-18-3533-2024

Revuelto, J., Lecourt, G., Lafaysse, M., Zin, I., Charrois, L., Vionnet, V., Dumont, M., Rabatel, A., Six, D., Condom, T., Morin, S., Viani, A., Sirguey, P., 2018. Multi-Criteria Evaluation of Snowpack Simulations in Complex Alpine Terrain Using Satellite and In Situ Observations. Remote Sens. 10, 1171. https://doi.org/10.3390/rs10081171

Reynolds, D., Quéno, L., Lehning, M., Jafari, M., Berg, J., Jonas, T., Haugeneder, M., Mott, R., 2024. Seasonal snow–atmosphere modeling: let's do it. The Cryosphere 18, 4315–4333. https://doi.org/10.5194/tc-18-4315-2024

Roussel, L., Dumont, M., Gascoin, S., Monteiro, D., Bavay, M., Nabat, P., Ezzedine, J.A., Fructus, M., Lafaysse, M., Morin, S., Maréchal, E., 2024. Snowmelt duration controls red algal blooms in the snow of the European Alps. Proc. Natl. Acad. Sci. 121, e2400362121. https://doi.org/10.1073/pnas.2400362121

Roussel, L., Dumont, M., Réveillet, M., Six, D., Kneib, M., Nabat, P., Fourteau, K., Monteiro, D., Gascoin, S., Thibert, E., Rabatel, A., Sicart, J.-E., Bonnefoy, M., Piard, L., Laarman, O., Jourdain, B., Fructus, M., Vernay, M., Lafaysse, M., 2025. Saharan dust impacts on the surface mass balance of Argentière Glacier (French Alps). The Cryosphere 19, 5201–5230. https://doi.org/10.5194/tc-19-5201-2025

Rutter, N., Essery, R., Pomeroy, J., Altimir, N., Andreadis, K., Baker, I., Barr, A., Bartlett, P., Boone, A., Deng, H., Douville, H., Dutra, E., Elder, K., Ellis, C., Feng, X., Gelfan, A., Goodbody, A., Gusev, Y., Gustafsson, D., Hellström, R., Hirabayashi, Y., Hirota, T., Jonas, T., Koren, V., Kuragina, A., Lettenmaier, D., Li, W.-P., Luce, C., Martin, E., Nasonova, O., Pumpanen, J., Pyles, R.D., Samuelsson, P., Sandells, M., Schädler, G., Shmakin, A., Smirnova, T.G., Stähli, M., Stöckli, R., Strasser, U., Su, H., Suzuki, K., Takata, K., Tanaka, K., Thompson, E., Vesala, T., Viterbo, P., Wiltshire, A., Xia, K., Xue, Y., Yamazaki, T., 2009. Evaluation of forest snow processes models (SnowMIP2). J. Geophys. Res. Atmospheres 114. https://doi.org/10.1029/2008JD011063

Smyth, E.J., Raleigh, M.S., Small, E.E., 2022. The Challenges of Simulating SWE Beneath Forest Canopies are Reduced by Data Assimilation of Snow Depth. Water Resour. Res. 58, e2021WR030563. https://doi.org/10.1029/2021WR030563

https://doi.org/10.5194/egusphere-2026-1464
Preprint. Discussion started: 22 May 2026

Sourp, L., Gascoin, S., Jarlan, L., Pedinotti, V., Bormann, K.J., Baba, M.W., 2025. Evaluation of high-resolution snowpack simulations from global datasets and comparison with Sentinel-1 snow depth retrievals in the Sierra Nevada, USA. Hydrol. Earth Syst. Sci. 29, 597–611. https://doi.org/10.5194/hess-29-597-2025

Spandre, P., François, H., Verfaillie, D., Lafaysse, M., Déqué, M., Eckert, N., George, E., Morin, S., 2019a. Climate controls on snow reliability in French Alps ski resorts. Sci. Rep. 9, 8043. https://doi.org/10.1038/s41598-019-44068-8

Spandre, P., François, H., Verfaillie, D., Lafaysse, M., Déqué, M., Eckert, N., George, E., Morin, S., 2019b. Climate controls on snow reliability in French Alps ski resorts. Sci. Rep. 9, 8043. https://doi.org/10.1038/s41598-019-44068-8

Strasser, U., Warscher, M., Rottler, E., Hanzer, F., 2024. openAMUNDSEN v1.0: an open-source snow-hydrological model for mountain regions. Geosci. Model Dev. 17, 6775–6797. https://doi.org/10.5194/gmd-17-6775-2024

Vernay, M., Lafaysse, M., Monteiro, D., Hagenmuller, P., Nheili, R., Samacoïts, R., Verfaillie, D., Morin, S., 2022. The S2M meteorological and snow cover reanalysis over the French mountainous areas: description and evaluation (1958–2021). Earth Syst. Sci. Data 14, 1707–1733. https://doi.org/10.5194/essd-14-1707-2022

Viallon-Galinier, L., Hagenmuller, P., Lafaysse, M., 2020. Forcing and evaluating detailed snow cover models with stratigraphy observations. Cold Reg. Sci. Technol. 180, 103163. https://doi.org/10.1016/j.coldregions.2020.103163

Vincent, L., Lejeune, Y., Lafaysse, M., Boone, A., Le Gac, E., Coulaud, C., Freche, G., Sicart, J.-E., 2018. Interception of snowfall by the trees is the main challenge for snowpack simulations under forests.

Vionnet, V., Leroux, N.R., Fortin, V., Abrahamowicz, M., Woolley, G., Mazzotti, G., Gaillard, M., Lafaysse, M., Royer, A., Domine, F., Gauthier, N., Rutter, N., Derksen, C., Bélair, S., 2025. Enhancing simulations of snowpack properties in land surface models with the Soil, Vegetation and Snow scheme v2.0 (SVS2). Geosci. Model Dev. 18, 9119–9147. https://doi.org/10.5194/gmd-18-9119-2025

Webster, C., Essery, R., Mazzotti, G., Jonas, T., 2023. Using just a canopy height model to obtain lidar-level accuracy in 3D forest canopy shortwave transmissivity estimates. Agric. For. Meteorol. 338, 109429. https://doi.org/10.1016/j.agrformet.2023.109429

Webster, C., Ginzler, C., Marty, M., Nussbaumer, A., Mazzotti, G., Jonas, T., 2025. Hourly potential light availability maps at 10 m resolution over Switzerland. Sci. Data 12, 1882. https://doi.org/10.1038/s41597-025-06152-9

Woolley, G.J., Rutter, N., Wake, L., Vionnet, V., Derksen, C., Essery, R., Marsh, P., Tutton, R., Walker, B., Lafaysse, M., Pritchard, D., 2024. Multi-physics ensemble modelling of Arctic tundra snowpack properties. The Cryosphere 18, 5685–5711. https://doi.org/10.5194/tc-18-5685-2024

Ylönen, M., Marttila, H., Geissler, J., Kuzmin, A., Korpelainen, P., Kumpula, T., Ala-Aho, P., 2025. UAV LiDAR surveys and machine learning improve snow depth and water equivalent estimates in boreal landscapes. The Cryosphere 19, 4585–4610. https://doi.org/10.5194/tc-19-4585-2025